

Published in final edited form as:

Sci Transl Med. ; 13(580): . doi:10.1126/scitranslmed.abd7064.

Nicotinamide for the treatment of heart failure with preserved ejection fraction*

Mahmoud Abdellatif¹, Viktoria Trummer-Herbst¹, Franziska Koser², Sylvère Durand^{3,4}, Rui Adão^{1,5}, Francisco Vasques-Nóvoa⁵, Johanna K. Freundt², Julia Voglhuber^{1,6}, Maria-Rosaria Pricolo⁷, Michael Kasa¹, Clara Türk^{8,9}, Fanny Aprahamian^{3,4}, Elías Herrero-Galán⁷, Sebastian J. Hofer¹⁰, Tobias Pendl¹⁰, Lavinia Rech¹, Julia Kargl¹¹, Nathaly Anto-Michel¹, Senka Ljubojevic-Holzer^{1,6}, Julia Schipke¹², Christina Brandenberger¹², Martina Auer^{13,14}, Renate Schreiber¹⁰, Chintan N. Koyani¹, Akos Heinemann¹¹, Andreas Zirlik¹, Albrecht Schmidt¹, Dirk von Lewinski¹, Daniel Scherr¹, Peter P. Rainer^{1,6}, Julia von Maltzahn¹⁵, Christian Mühlfeld¹², Marcus Krüger^{8,9}, Saša Frank^{16,13}, Frank Madeo^{6,10}, Tobias Eisenberg^{6,10}, Andreas Prokesch^{6,13,14}, Adelino F. Leite-Moreira⁵, André P. Lourenço⁵, Jorge Alegre-Cebollada⁷, Stefan Kiechl^{16,17}, Wolfgang A. Linke², Guido Kroemer^{3,4,18,19,20,#}, Simon Sedej^{1,6,21,#}

¹Department of Cardiology, Medical University of Graz, Graz 8036, Austria

²Institute of Physiology II, University of Münster, Münster 48149, Germany

³Metabolomics and Cell Biology Platforms, Institut Gustave Roussy, Villejuif 94805, France

⁴Centre de Recherche des Cordeliers, Equipe labellisée par la Ligue contre le cancer, Université de Paris, Sorbonne Université, INSERM U1138, Institut Universitaire de France, Paris 75006, France

⁵Department of Surgery and Physiology, Cardiovascular Research and Development Centre (UnIC), Faculty of Medicine, University of Porto, Porto 4200-319, Portugal

⁶BioTechMed Graz, Graz 8010, Austria

⁷Centro Nacional de Investigaciones Cardiovasculares (CNIC), Madrid 28029, Spain

⁸Institute for Genetics, Cologne Excellence Cluster on Cellular Stress Responses in Aging-Associated Diseases, Cologne 50931, Germany

⁹Center for Molecular Medicine (CMMC), University of Cologne, Cologne 50931, Germany

#Corresponding author. simon.sedej@medunigraz.at (S.S.), kroemer@orange.fr (G.K.).

*This manuscript has been accepted for publication in Science Translational Medicine. This version has not undergone final editing. Please refer to the complete version of record at www.sciencetranslationalmedicine.org/. The manuscript may not be reproduced or used in any manner that does not fall within the fair use provisions of the Copyright Act without the prior written permission of AAAS.

Author contributions: M. Abdellatif and S.S. designed and supervised the study; M. Abdellatif, S.S. and G.K. wrote the manuscript; M. Abdellatif, V.T.-H., F.K., S.D., R.A., F.V.-N., J.K.F., J.V., M.-R.P., M.K., C.T., F.A., E.H.-G., S.J.H., T.P., L.R., J.K., N.A.-M., S.L.-H., J.S., C.B., M. Auer, R.S., C.N.K., J.v.M., S.S. performed experiments and analyzed and discussed data; D.v.L., P.P.R., D.S. characterized patients and provided human cardiac tissue and data; A.H., A.S., C.M., M.K., S.F., T.E., F.M., A.Z., A.P., A.F.L.-M., A.P.L., J.A.-C., S.K., W.A.L., G.K. discussed and analyzed data and/or gave conceptual advice.

Competing interests: M. Abdellatif, T.E., F.M. and S.S. are involved in a patent application related to the cardiometabolic effects of nicotinamide.

- ¹⁰Institute of Molecular Biosciences, University of Graz, NAWI Graz, Graz 8010, Austria
- ¹¹Otto Loewi Research Center, Division of Pharmacology, Medical University of Graz, Graz 8010, Austria
- ¹²Institute of Functional and Applied Anatomy, Hannover Medical School, Hannover 30625, Germany
- ¹³Gottfried Schatz Research Center for Cell Signaling, Metabolism and Aging, Medical University of Graz, Graz 8010, Austria
- ¹⁴Division of Cell Biology, Histology and Embryology, Medical University of Graz, Graz 8010, Austria
- ¹⁵Leibniz Institute on Aging, Jena 07745, Germany
- ¹⁶Department of Neurology, Medical University of Innsbruck, Innsbruck 6020, Austria
- ¹⁷VASCage, Research Centre for Promoting Vascular Health in the Ageing Community, Innsbruck 6020, Austria
- ¹⁸Pôle de Biologie, Hôpital Européen Georges Pompidou, AP-HP, Paris 75015, France
- ¹⁹Suzhou Institute for Systems Medicine, Chinese Academy of Sciences, Suzhou 215000, China
- ²⁰Karolinska Institute, Department of Women's and Children's Health, Karolinska University Hospital, Solna 17164, Sweden
- ²¹Faculty of Medicine, University of Maribor, Maribor 2000, Slovenia

Abstract

Heart failure with preserved ejection fraction (HFpEF) is a highly prevalent and intractable form of cardiac decompensation commonly associated with diastolic dysfunction. Here, we show that diastolic dysfunction in patients with HFpEF is associated with a cardiac deficit in nicotinamide adenine dinucleotide (NAD⁺). Elevating NAD⁺ by oral supplementation of its precursor, nicotinamide, improved diastolic dysfunction induced by aging (in 2-year-old C57BL/6J mice), hypertension (in *Dahl* salt-sensitive rats) or cardiometabolic syndrome (in ZSF1 obese rats). This effect was mediated partly through alleviated systemic comorbidities and enhanced myocardial bioenergetics. Simultaneously, nicotinamide directly improved cardiomyocyte passive stiffness and calcium-dependent active relaxation through increased deacetylation of titin and the sarcoplasmic reticulum calcium ATPase 2a, respectively. In a long-term human cohort study, high dietary intake of naturally occurring NAD⁺ precursors was associated with lower blood pressure and reduced risk of cardiac mortality. Collectively, these results suggest NAD⁺ precursors, and especially nicotinamide, as potential therapeutic agents to treat diastolic dysfunction and HFpEF in humans.

Introduction

Heart failure with preserved ejection fraction (HFpEF) is a prevalent form of cardiac decompensation that is increasing with population aging (1). At variance with heart failure with reduced ejection fraction (HFrEF), there are still no evidence-based therapies for

HFpEF (2), although it is the leading cause of hospitalization in the elderly with almost a third of discharged patients being readmitted or dying within 3 months (3). The quest for effective HFpEF pharmacotherapies has been frustrated by the heterogeneous nature of the disease, which is increasingly recognized as an age-related systemic syndrome (4). Although inflammation and nitrosative/oxidative stress have been proposed to contribute to HFpEF pathogenesis (5, 6), the full range of mechanisms underlying HFpEF remains far from being completely understood. The complexity of HFpEF is further underscored by sex-related differences. Women tend to have a worse quality of life despite higher overall survival than men with HFpEF (7), which further thwarts a rationally designed therapy.

Since previous efforts using HFpEF medications (*e.g.*, neurohormonal antagonists and nitrate derivatives) failed to improve premature mortality in patients with HFpEF (8), emerging anti-aging therapies that may target common HFpEF abnormalities are worth considering. Indeed, caloric restriction, the most effective longevity-promoting intervention in model organisms (9), has been shown to improve left ventricular hypertrophy and exercise capacity in men and women with HFpEF (10). However, implementing caloric restriction in humans is limited due to the lack of compliance and potential adverse effects on bone density and immunity (9).

The beneficial effects of caloric restriction can be mimicked, at least in part, through increasing nicotinamide adenine dinucleotide (NAD⁺) cellular concentrations (11, 12). Restoring NAD⁺ abundance attenuates metabolic abnormalities in animal models of aging and obesity (13), which are also two major risk factors for HFpEF (2). Interestingly, experimental HFpEF is associated with perturbations in fatty acid oxidation, redox reactions, mitochondrial electron transfer, and ATP synthesis (14), which are all NAD⁺-dependent processes. Thus, it is plausible that NAD⁺ metabolism is deranged in HFpEF, and that it might be therapeutically targeted. Driven by this speculation, we examined whether supplementation of the NAD⁺ precursor nicotinamide (NAM) attenuated diastolic dysfunction, a common cardiac abnormality in clinical HFpEF, using animal models of aging, hypertension, and metabolic syndrome.

Here, we report that patients with HFpEF and animals with diastolic dysfunction exhibit a deficit in cardiac NAD⁺. NAM administration to animals with typical HFpEF risk factors substantially improved diastolic dysfunction. This effect was mediated at least in part through increased deacetylation of the proteins regulating the mechanoelastic properties of cardiac myocytes. Concurrently, NAM enhanced energy metabolism, thereby improving myocardial and skeletal muscle bioenergetics. Finally, in a prospective human cohort, dietary intake of NAD⁺ precursors was associated with lower blood pressure and reduced risk of cardiac mortality.

Results

Elevating NAD⁺ improves diastolic dysfunction in ZSF1 obese rats

We first quantified NAD⁺ in hyperphagic leptin receptor-deficient ZSF1 rats, a model of metabolic syndrome and HFpEF (15, 16). These obese, diabetic and hypertensive rats replicate many aspects of clinical HFpEF, including diastolic dysfunction, effort

intolerance and lung congestion, despite having preserved ejection fraction (15, 16). As compared to lean controls, ZSF1 obese rats had lower cardiac and hepatic NAD⁺, despite similar expression of the rate-limiting enzyme in the NAD⁺ salvage pathway, nicotinamide phosphoribosyltransferase (NAMPT), which converts NAM to NAD⁺ (fig. S1).

Since NAMPT expression was preserved in ZSF1 obese rats, we opted to administer the NAD⁺ precursor NAM (40 mM in the drinking water, Fig. 1A) to test whether boosting NAD⁺ improves diastolic dysfunction. Both male and female rats were included to capture possible sex-related differences. NAM supplementation increased NAM and NAD⁺ in the heart and liver, and circulating NAM in plasma (fig. S1, A to C), while it induced substantial improvements in the cardiac phenotype in vivo. Both male and female NAM-treated rats exhibited less cardiac hypertrophy and unaltered ejection fraction (Fig. 1, B to D and table. S1). Importantly, NAM reduced the echocardiography-derived E/e' ratio, a non-invasive measure of left ventricular (LV) diastolic dysfunction, to values comparable to those observed in leptin receptor-sufficient lean rats (Fig. 1, E and F). Such improvement in diastolic dysfunction was further corroborated in both sexes by invasive determination of LV end-diastolic pressure, which was elevated in obese compared to lean controls, and normalized by NAM (Fig. 1G). Enhanced diastolic function upon NAM supplementation correlated with faster LV active relaxation, as demonstrated by a shorter LV pressure decay time constant τ (table. S2), and with reduced LV passive stiffness, as indicated by the lower myocardial stiffness constant β and the downward-shift of the end-diastolic pressure-volume relationship (Fig. 1, H to J).

The improved cardiac phenotype of NAM-treated rats was accompanied by a reduced lung weight-to-tibia length ratio, a measure of pulmonary congestion and a clinical sign of heart failure in rodent models (Fig. 1K). Moreover, exercise tolerance testing coupled to indirect calorimetry revealed that NAM enhanced maximal oxygen consumption, running distance and workload, indicating that NAM improved the cardiopulmonary functional capacity of ZSF1 obese rats (Fig. 1, L to N). Collectively, these results indicate that NAM supplementation attenuates structural and functional cardiac abnormalities reminiscent of HFpEF in male and female ZSF1 obese rats.

NAM alleviates HFpEF risk factors in ZSF1 obese rats

We then examined whether NAM affects other comorbidities in ZSF1 obese rats, including hypertension, diabetes and obesity, which are also common risk factors for HFpEF in patients (2). NAM reduced systolic, diastolic and mean blood pressure (Fig. 2, A and B, and fig. S2, A to D). This antihypertensive effect correlated with improved endothelial function, as indicated by an enhanced vasodilatory response to acetylcholine in isolated aortic rings (Fig. 2, C to D, and fig. S2, E and F). At variance with a previous report on high-fat diet-induced obesity (13), NAM did not improve glucose homeostasis or insulin sensitivity in hyperphagic ZSF1 obese rats (fig. S3). However, NAM conspicuously reduced body weight gain and visceral fat accumulation (Fig. 2, E to G) without affecting lean body mass (fig. S4A), indicating improved body composition. Although NAM did not reduce food intake (fig. S4B), it attenuated body weight gain per consumed *kcal* of energy (*i.e.*, feeding efficiency; Fig. 2H). Consistently, NAM increased daily energy expenditure and oxygen

consumption independently of body mass or circadian variations (Fig. 2, I and J, and fig. S5). Hence, reduced adiposity by NAM can be attributed to increased energy expenditure rather than reduced calorie intake. Finally, NAM-treated ZSF1 obese rats exhibited reduced adipose tissue infiltration by leukocytes including B, T and natural killer cells, though without changes in macrophages (fig. S6). In sum, NAM improved systemic HFpEF risk factors, including obesity and hypertension, to a comparable extent in male and female ZSF1 obese rats.

NAM-induced metabolic reprogramming reinstates myocardial energy supplies in HFpEF

To elucidate the impact of NAM on general metabolism, we performed unbiased metabolomic profiling of plasma from fasted ZSF1 rats. To determine underlying rather than compensatory alterations, we used 12-week-old rats that did not yet exhibit morbid obesity or fully developed heart failure. NAM-treated ZSF1 obese rats displayed substantial metabolic reprogramming (Fig. 3A), thereby resembling the metabolomic profile of lean controls (Fig. 3B). A total of 44% of detectable metabolites ($n=82/187$) – mostly fatty and amino acids – were differentially regulated in response to NAM supplementation (Fig. 3C). NAM reduced branched-chain amino acids and their keto acid derivatives as well as glycolytic intermediates (Fig. 3D). In contrast, NAM augmented fatty acids that were predominantly (poly)-unsaturated as well as acyl-carnitines and 3-hydroxybutyrate (Fig. 3E and fig. S7, A and B), which may reflect increased lipolysis, as also suggested by high glycerol abundance (fig. S7C) and reduced adiposity in treated ZSF1 obese rats.

We next sought to determine how this systemic metabolic shift (fig. 7D) affect cardiac metabolism. Comparative analysis of cardiac transcriptome in treated *versus* untreated ZSF1 obese rats revealed tricarboxylic acid (TCA) cycle as the most enriched pathway (fig. S8, A to C) in the heart. Several TCA cycle metabolites and genes were increased in NAM-supplemented rats (Fig. 3, F and G). NAM also induced multiple genes related to oxidative phosphorylation (fig. S8D), which was coupled to increased ATP/ADP and phosphocreatine/ATP ratios in the left ventricle (Fig. 3H). Thus, NAM partially restored constrained myocardial energy reserves in ZSF1 obese rats. Similarly, NAM increased ATP and phosphocreatine levels in skeletal muscle (Fig. 3I), but without detectable improvements in skeletal myofiber size or the amount of regenerating myofibers (fig. S9). Taken together, the switch from glycolytic to a more energy-efficient oxidative metabolism in NAM-treated ZSF1 obese rats (Fig. 3J) coincides with the reversal of bioenergetic abnormalities that are closely linked to diastolic dysfunction in clinical HFpEF (17).

NAM improves cardiomyocyte relaxation and stiffness in vitro

Beyond its pivotal role in energy metabolism, NAD⁺ is an important signaling molecule involved in protein deacetylation through the sirtuin family of deacetylases (18). In line with previous reports (13, 19), NAM-treated rats showed increased cardiac expression of the NAD⁺-dependent deacetylase SIRT1 (fig. S10). However, the effect of NAM on sirtuin activity is complex, and available evidence is rather inconclusive as to whether NAM supplementation enhances or reduces protein acetylation (13). Therefore, we performed a comprehensive acetylome analysis of myocardia from untreated and NAM-treated ZSF1 rats. Unexpectedly, the total number of acetylated proteins and the global degree of

acetylation were comparable among the groups (Fig. 4, A and B, and fig. S11). However, subcellular analysis revealed a disproportionate number of non-mitochondrial peptides that were modestly deacetylated in NAM-treated ZSF1 obese rats (Fig. 4B). Therefore, we focused our analysis on the proteins directly regulating the mechanoelastic properties of cardiomyocytes.

First, we examined the acetylation status of sarcoplasmic reticulum Ca^{2+} transport ATPase 2a (SERCA2a), a key protein regulating active relaxation of cardiomyocytes through Ca^{2+} reuptake into the sarcoplasmic reticulum (20). As compared to ZSF1 lean rats, obese rats showed a non-significant ($P=0.118$) increase in SERCA2a (*Atp2a3*) acetylation (fig. S11), which was markedly reduced by NAM (Fig. 4C). Deacetylation of SERCA2a is known to improve its pump activity (21), and thus might contribute to improved diastolic function through enhanced active relaxation of cardiomyocytes. To examine this possibility, we measured Ca^{2+} transients and sarcomere shortening in isolated cardiomyocytes from NAM-treated ZSF1 obese rats, which showed faster Ca^{2+} reuptake and sarcomere re-lengthening as compared to control ZSF1 obese rats (fig. S12). To exclude the secondary effects of improved hypertension and general metabolism, we incubated single cardiomyocytes of non-treated ZSF1 obese rats with NAM for one hour. Acute NAM treatment reproduced the effects of chronic NAM administration (fig. S12), including enhanced Ca^{2+} transient amplitude and Ca^{2+} reuptake, as well as ameliorated sarcomere shortening and re-lengthening (*i.e.*, relaxation) (Fig. 4, D to I), suggesting that NAM improved cardiac relaxation at least in part through direct effects on cardiomyocytes.

Second, we examined the acetylation status of titin, a large sarcomeric protein that determines passive stiffness of cardiomyocytes (22). We detected five lysine residues in titin that were all but one significantly deacetylated by NAM administration (Fig. 4C). However, unlike other post-translational modifications of titin (22), it remains unknown as to whether deacetylation alters the mechanical properties of titin or cardiomyocytes. To address this point, we measured cardiomyocyte passive stiffness in NAM-treated and control ZSF1 rats. In line with the *in vivo* effect on myocardial passive stiffness, skinned cardiomyocytes from NAM-treated rats exhibited improved passive tension as compared to those from non-treated ZSF1 obese rats (Fig. 5A). We then performed a comprehensive biochemical analysis of titin, which revealed that NAM did not affect titin isoform composition (the proportion of the stiff N2B isoform), phosphorylation of the major N2B titin species, or titin oxidation (fig. S13). Thus, reduced cardiomyocyte stiffness in NAM-treated ZSF1 obese rats was specifically associated with titin deacetylation (Fig. 4C and Fig. 5B). However, titin acetylation was not remarkably higher in ZSF1 obese *vs.* lean rats (Fig. 5B and fig. S11). Therefore, to determine the functional relevance of titin deacetylation, we isolated rat cardiomyocytes and then skinned and incubated them with recombinant SIRT1 protein. This approach effectively deacetylated the stiff N2B titin isoform *in vitro* (Fig. 5C), and resulted in clearly reduced titin-based cardiomyocyte passive tension (Fig. 5D). Hence, although increased titin acetylation does not seem to be a prerequisite for diastolic dysfunction, its deacetylation is sufficient to improve cardiomyocyte elasticity. Taking into account that NAM did not reduce cardiac fibrosis (Fig. 5, E and F), the reduced myocardial stiffness in NAM-treated ZSF1 obese rats might be attributed to titin deacetylation. Altogether, these results indicate that in addition to the beneficial effects on energy metabolism, NAM

might ameliorate diastolic function also through titin and SERCA2a deacetylation, leading to improved passive stiffness and calcium-dependent active relaxation of cardiomyocytes, respectively.

NAM improves diastolic dysfunction in hypertensive rats and aged mice

Although our in vitro results suggest that cardiomyocyte-specific effects of NAM contribute to improved diastolic dysfunction, it is possible that the in vivo effects of NAM on ZSF1 obese rats are secondary to the reduction in adiposity. To test whether NAM ameliorates diastolic function also in the absence of obesity, we used two non-obese models of diastolic dysfunction induced by hypertension or advanced age, which are also predominant HFpEF risk factors (2). *Dahl* salt-sensitive rats were fed a high-salt diet for 5 weeks until they developed hypertensive cardiomyopathy (23). Then, the rats received a low-salt diet combined (or not) with adjunct NAM in the drinking water (Fig. 6A). Unlike in ZSF1 obese rats, NAM modestly reduced salt-induced hypertension in *Dahl* rats (Fig. 6, B to D). Of note, NAM effectively ameliorated diastolic dysfunction, as assessed by echocardiography and invasive LV end-diastolic pressure measurements (Fig. 6, E to I). Consistently, NAM-treated *Dahl* rats exhibited reduced cardiac hypertrophy and pulmonary congestion (Fig. 6J), which was associated with improved cardiopulmonary functional capacity and exercise tolerance as compared to controls (Fig. 6, K to M). We considered the possibility that the antihypertensive effect of NAM, albeit modest, might have contributed to the cardioprotective effects observed in NAM-treated *Dahl* rats. However, after correcting for the difference in systolic blood pressure between the groups using Analysis of Covariance (ANCOVA), end-diastolic pressure and hypertrophy were still significantly improved (Bonferroni-corrected P value = 0.037 and 0.008, respectively), suggesting that other mechanisms than a reduction in blood pressure must be involved in the beneficial action of NAM. Indeed, although total acetylated SERCA2a and acetylated titin were not altered in *Dahl* rats (Fig. 6, N and O), NAM treatment of *Dahl* rats improved cardiac energy metabolism, with higher cardiac ATP/ADP ratios, coupled to an increased availability of unsaturated fatty acids (Fig. 6P).

Next, we tested the effect of NAM in 24-month-old C57BL/6J mice, a model of age-related diastolic dysfunction (24). These mice are normotensive and non-obese and, thus, allow us to examine diastolic dysfunction in the absence of other risk factors than age (25). Aged mice received NAM for 4 months in the drinking water (Fig. 7A), and were then subjected to cardiometabolic phenotyping. As compared to controls, NAM-treated aged mice exhibited no alterations in ejection fraction, but lower heart weight-to-tibia length ratios, denoting reduced hypertrophy (Fig. 7, B to D). Importantly, NAM improved the age-related decline in diastolic function, as indicated by a lower E/e' ratio and a shorter isovolumic relaxation time (Fig. 7, E to G), but without changes in lung weight (fig. S14A). In line with the observations made in ZSF1 obese rats, improved diastolic function in NAM-treated aged mice was associated with total SERCA2a and titin deacetylation (Fig. 7, H and I), albeit non-significantly (P values = 0.067 and 0.051, respectively). Notably, NAM induced cardioprotection in aged mice without any alterations in body weight, food intake or glucose tolerance (fig. S14, B to D). Based on these findings, we conclude that NAM can ameliorate

diastolic dysfunction, independently from its anti-obesity and anti-hypertensive effects, *via* enhanced energy metabolism and/or deacetylation of SERCA2a and titin.

NAD⁺ supply is associated with lower risk of HFpEF and cardiac mortality in humans

To determine the clinical relevance of our findings, we examined the relationship between dietary intake of naturally occurring NAD⁺ precursors and cardiovascular health and survival in humans. The main dietary sources of NAD⁺ are NAM and nicotinic acid, collectively referred to as preformed niacin. However, NAD⁺ can also be synthesized *de novo* using tryptophan. Thus, the total dietary supply of NAD⁺ - known as niacin equivalents (NE) - is calculated as follows: preformed niacin *plus* tryptophan divided by 60 (26). In the prospective population-based Bruneck cohort (27), we found higher nutritional intake of these NAD⁺ precursors (evaluated by food questionnaires) to be associated with a lower risk of all-cause death during the 20-year follow-up period (Fig. 8A). This association was driven by, and specific for, cardiac mortality (a composite of deaths from heart failure, myocardial infarction and sudden cardiac death) (Fig. 8A). Other causes of death emerged as unrelated (non-cardiac vascular death: hazard ratio [95% CI] from multivariable models, 1.02 [0.79-1.33] *P*value = 0.88 for preformed niacin, and 1.10 [0.85-1.42] *P*=0.46 for NE; cancer death: 0.88 [0.71-1.09] *P*=0.25 and 0.86 [0.70-1.07] *P*=0.17; and other causes of death: 0.88 [0.72-1.07] *P*=0.109 and 0.96 [0.79-1.16] *P*=0.66). Furthermore, the dietary intake of NAD⁺ precursors inversely correlated with systolic blood pressure (Fig. 8B). Importantly, these associations held true after correcting for caloric intake and other potential confounding factors, including age, sex, smoking, diabetes, alcohol intake, body-mass index and total cholesterol, as well as composite categories of food items, macronutrients and the Alternative Healthy Eating Index. The potential benefits tended, albeit not significantly, to be more evident in women compared to men. Notably, the average (interquartile range, IQR) NE intake was 28.9 mg (23.5-35.0) and 26.9 mg (21.9-33.0) in men and women, respectively, which is much higher than the daily intake (14-16 mg) required for the avoidance of hypovitaminosis (26). Hence, these associations are likely driven by the benefits of increased NAD⁺ precursors intake rather than adverse effects of niacin/vitamin B₃ deficiency.

While the Bruneck Study has long-term and 100% complete follow-up, represents the general (local) community, and includes the assessment of multiple medical and socioeconomic characteristics of each individual along with the detailed characterization of dietary intakes based on dietician-administered and validated food frequency questionnaires (table. S3), it has limitations. These include a potential residual confounding influence by other nutritional ingredients or dietary patterns linked to NAD⁺ precursor intake, and the use of surrogate endpoints rather than HFpEF itself, as widely-accepted diagnostic algorithms for HFpEF were not available until recently (28, 29). Therefore, to substantiate the translational potential of our study, we quantified NAD⁺ in human LV biopsies obtained from donor hearts with HFpEF compared to those with no cardiac abnormalities, but similar demographics and associated comorbidities (table. S4). Although these patients did not exhibit a severe HFpEF phenotype, they had lower cardiac NAD⁺ than non-failing donors (Fig. 8C). Interestingly, diminished NAD⁺ was not associated with reduced expression of NAMPT (fig. S15) – the rate-limiting enzyme in the NAD⁺ salvage pathway – as previously

reported for patients with HFrEF (30). However, we detected reduced circulating amount of NAM in the plasma samples of these patients (Fig. 8D), suggesting that, similar to animal models of diastolic dysfunction, patients with HFpEF might benefit from NAM supplementation. That said, we acknowledge that although these donor hearts fulfilled the echocardiographic criteria for HFpEF with NT-proBNP concentrations that were on average 8-fold higher than the threshold to diagnose HFpEF, data on the signs and symptoms were not always available at the time of death/donation due to the acute course of disease in some patients. Hence, further clinical studies are warranted to corroborate these observations.

Discussion

HFpEF is a complex and multifaceted systemic disease, which lacks evidence-based therapies. As such, limited understanding of HFpEF pathogenesis hinders the development of effective therapies that would reduce hospitalizations and premature mortality in patients with HFpEF. Due to the ongoing debate regarding which animal model best recapitulates the heterogeneity of human HFpEF, we used three different animal models of diastolic dysfunction, a clinical hallmark of HFpEF, caused by morbid obesity, salt-sensitive hypertension or old age. In all three models, oral supplementation of NAM effectively improved diastolic dysfunction.

Mechanistically, the cardioprotective impact of NAM on diastolic function appeared to be mediated through mutually non-exclusive NAD⁺ effects on systemic energy metabolism and on cardiomyocyte local signaling. Particularly under conditions of metabolic and hemodynamic stress, like cardiometabolic syndrome, NAM had a major impact on adiposity and hypertension, which might contribute to improved diastolic dysfunction through reinstating muscle bioenergetics and alleviating cardiac afterload, respectively (17, 31). However, the beneficial effect of NAM on diastolic dysfunction was also evident in the absence of obesity and hypertension, as observed in aged mice, suggesting that NAM might also act directly on the heart. Indeed, NAM improved active relaxation of single cardiomyocytes in vitro. This effect was mediated by enhanced Ca²⁺ reuptake into the sarcoplasmic reticulum through SERCA2a deacetylation in aged mice, restored ATP in hypertensive *Dahl* rats, or both in ZSF1 obese rats. Thus, elevating intracellular NAD⁺ concentrations by NAM supplementation exerts pleiotropic effects on energy metabolism and protein acetylation, which may independently contribute to better relaxation and mechanoelastic properties of cardiac myocytes, and consequently improve diastolic dysfunction (fig. S16).

Importantly, our results reveal NAM-triggered titin deacetylation as a potential mechanism regulating myocardial stiffness. Titin-based cardiomyocyte stiffness was improved in NAM-treated animals in the absence of other post-translational modifications of titin (*i.e.*, phosphorylation and oxidation), and without changes in titin isoform composition. Of note, titin deacetylation induced in vitro reduced cardiomyocyte stiffness in healthy cardiomyocytes, suggesting that titin deacetylation may be sufficient for improving cardiomyocyte elasticity. Future studies, however, will need to determine the most relevant titin acetylation sites regulating cardiomyocyte elasticity, and also to reconcile our findings with the reported improvement of diastolic dysfunction by histone deacetylase (HDAC)

inhibitors (32, 33). In this regard, our study does not exclude the possibility that deacetylation of other proteins and/or other NAD⁺-related reactions (*e.g.*, ADP-ribosylation) might contribute to NAM-mediated cardioprotection. Non-parenchymatous cells, including resident leukocytes, might also respond to NAD⁺, which has vast anti-inflammatory and immunomodulatory effects (34, 35). Thus, we cannot exclude that improved diastolic function by NAM might involve non-cell-autonomous effects related to the suppression of inflammation in HFpEF (5).

Notably, we show here that deacetylation of non-mitochondrial proteins plays a role in NAD⁺ effects on the heart, specifically in the setting of diastolic dysfunction and HFpEF. Prior NAD⁺-related studies, which focused on systolic dysfunction and HFrEF, have detected altered acetylation of mitochondrial proteins. In both human and mouse hearts with dilated cardiomyopathy, acetylproteome analysis revealed extensive acetylation of various mitochondrial protein lysine residues (36, 37). However, this finding was recently challenged in a genetic mouse model of dilated cardiomyopathy, where Diguët *et al.* (30) failed to detect altered acetylation of cardiac proteins.

Besides protein acetylation, the mode of NAD⁺ decline also seems to differ between HFrEF and HFpEF. As opposed to reduced NAMPT expression in HFrEF (30), cardiac NAMPT was preserved in HFpEF, both in humans and ZSF1 obese rats. This suggests that the HFpEF-related decline in NAD⁺ might be a consequence of an increased NAD⁺ demand, rather than reduced NAD⁺ salvage/biosynthesis, as proposed for HFrEF (30, 36). However, since NAD⁺ flux does not strongly correlate with the protein expression of its biosynthetic or consuming enzymes (38), this hypothesis will need to be properly tested in future studies using *in vivo* NAD⁺ flux measurements. That said, available flux measurements from aged mice, a well-established model of diastolic dysfunction, indicate that increased NAD⁺ consumption – not impaired production – causes the age-related NAD⁺ decline (39). This may have major implications for the choice of the optimal NAD⁺ precursor for either form of heart failure. We speculate that, in conditions with an intact NAD⁺ salvage pathway, like HFpEF, NAM might be a superior NAD⁺ precursor. In contrast, in HFrEF or similar conditions associated with reduced NAMPT expression, other NAD⁺ precursors like nicotinamide riboside might be more effective due to the compensatory increase in the nicotinamide riboside kinase pathway (30, 40).

Although NAD⁺ precursors are being tested in a variety of age-related disorders, there are currently no registered clinical trials examining their efficacy in HFpEF. Similarly, there are no available data on the effect of sirtuin activators, like resveratrol, in HFpEF, although a registered trial (NCT01185067) testing the effect of grape seed extract on HFpEF has been completed. To this end, our epidemiological analysis of a prospective cohort revealed that a diet enriched in NAD⁺ precursors, in the form of niacin (*i.e.*, the combination of NAM and nicotinic acid), is associated with lower blood pressure and a reduced risk of overall and cardiac mortality in humans. However, we acknowledge that this is a correlative observation and, albeit promising, should be interpreted with caution.

Taken together, the experimental and clinical evidence provided in this study lends support to NAD⁺ precursors, such as NAM, as potential therapeutic agents to treat diastolic

dysfunction and potentially HFpEF in humans. The human-equivalent for the NAM dose used in animals is ~2-3 g/day (for an average adult of 60-80 kg), which is clinically proven to be safe and is tolerable in cardiac patients (41). NAM is also orally bioavailable, thereby reaching the blood circulation in significant amounts to boost NAD⁺ metabolism throughout the body (38). Thus, interventional studies in patients are warranted to test whether NAM will be an effective therapy for clinical HFpEF, which affects at least 50% of heart failure patients and arguably represents one of the toughest challenges in cardiovascular medicine (2, 8).

Materials and Methods

Study design

The aim of this study was to investigate the role of NAD⁺ in diastolic dysfunction and HFpEF. We quantified cardiac NAD⁺ in patients with HFpEF and animals with diastolic dysfunction. Furthermore, we evaluated the association between dietary intake of naturally occurring NAD⁺ precursors and cardiac mortality in a long-term human cohort. To examine the effect of increasing cellular NAD⁺ abundance on diastolic dysfunction *in vivo*, the NAD⁺ precursor NAM was orally supplemented to aged C57BL/6J mice, *Dahl* salt-sensitive rats and ZSF1 obese rats, which model three key risk factors for HFpEF, namely aging, hypertension and metabolic syndrome, respectively. We applied a multitude of *in vivo* and *in vitro* assays, including invasive hemodynamics, echocardiography, exercise tolerance testing with indirect calorimetry, RNA sequencing, metabolome profiling, and myocardial bioenergetics. Furthermore, titin mechanics and simultaneous calcium photometry and sarcomere shortening measurements were performed in isolated cardiomyocytes. Sample sizes were empirically determined based on our previous experience with the animal models used (24, 42). All animals were randomly allocated to the treatment groups, which were stratified for body weight, and the experimenters were blinded to such allocation. The exact number of animals and replications in each experiment is provided in the respective figure legend. Please refer to Supplementary Materials and Methods for further details on experimental procedures, uncropped scans of representative immunoblots (fig. S17) and detailed metabolomics data (table S5). Raw data are either presented as individual data points in the graphs or reported in data file S1.

Statistical analysis

Data are presented as bar or line graphs with error bars showing mean and SEM, respectively, with single data points superimposed. Indicated sample size in figure legends refer to biological replicates (*ie*, independent animals or isolated primary cardiomyocytes thereof). Comparisons between two groups were done by Welch t-test. In case of multiple group comparisons, ANOVA followed by Dunnett's or Bonferroni post-hoc testes were applied. For factorial designs including multiple genotypes, genders, and treatments, a linear mixed model was used including these as fixed factors, and the cohort as a random factor in case if an outcome was tested in multiple cohorts. For end-systolic and end-diastolic pressure volume relationships comparisons, the corresponding coefficient in the fitting equation was included as a covariate (*ie*, α for EDPVR β and V_0 for ESPVR Ees). In case of serial measurements (*e.g.*, body weight and blood pressure), Greenhouse-Geisser-

corrected two-way repeated measures ANOVA was used. Generally, significant factorial designs were followed by pairwise comparisons that were corrected in case of multiple comparisons by Bonferroni or Dunnett's post hoc. Data residuals distribution was confirmed by Shapiro-Wilk's test, while homogeneity of variance was verified by Levene's test or Brown-Forsythe test, depending on distribution. In case of ANCOVAs, homogeneity of regression slopes between the groups was also confirmed. Data violating the assumptions were either transformed or alternative tests were used as appropriate. This included Mann-Whitney test for comparisons of two groups violating normality of distribution, and Welch's test with Games-Howell post-hoc test for comparisons of multiple groups with heterogeneous variances.

As for the human epidemiological data, niacin and niacin equivalent intakes were adjusted for total caloric intake by using the residual method (43). They were then scaled to unit variance such that effects were estimated for a one-standard deviation increase in niacin and niacin equivalent intake. Outcome analyses on death employed cox proportional hazards models to estimate hazard ratios (HRs) and 95% confidence intervals (95% CIs). No departure from the proportional hazards assumption was detected when inspecting Schoenfeld residuals and checking the parallelity of log-log survival plots. All analyses were adjusted for caloric intake (M1). Multivariable analyses additionally included age, sex, current smoking, diabetes, alcohol intake, hypertension, body-mass index, and total cholesterol (M2). Sensitivity analyses additionally adjusted for composite categories of food items, macronutrients, and the Alternative Healthy Eating Index. Analyses on blood pressure employed linear regression analysis and used the same adjustment. Analyses were conducted with SPSS 26.0 (SPSS Inc, Chicago, USA) and R 3.6.0 (R Foundation for Statistical Computing, Vienna, Austria).

Statistical analysis of omics data and indirect calorimetry metabolic studies are described in detail within their respective methods sections in Supplementary Materials and Methods. All reported *P* values are two-sided and an alpha level of 0.05 was used throughout. Unless stated otherwise, statistical analyses were performed using IBM SPSS statistics software (Version 25) or GraphPad Prism 8 (GraphPad Software, LLC, Massachusetts, USA).

Supplementary Material

Refer to Web version on PubMed Central for supplementary material.

Acknowledgements

The authors are grateful to M. Lechleitner, N. Vicente, N. Djalina, M. Agreiter, A. Humnig and F. Kaufmann for their excellent technical assistance, and Graz Biobank. The authors are indebted to B. Obermüller and the animal facility staff of the Institute of Biomedical Research (IBF, Medical University of Graz) for wellbeing of our animals.

Funding

this study was thankfully supported by the European Research Area Network on Cardiovascular Diseases (ERA-CVD) through the MINOTAUR consortium: S.S. (The Austrian Science Fund – FWF, I3301-B31), G.K. (Agence Nationale de la Recherche – ANR), W.A.L. (Bundesministerium für Bildung und Forschung – BMBF), J.A.C. (Instituto de Salud Carlos III – ISCIII, AC16/00045) and A.L.M. (Portuguese Foundation for Science and Technology – FCT). M. Abdellatif acknowledges funding received from the European Society of Cardiology in

form of an ESC Research Grant and from the Austrian Society of Cardiology (Präsidentenstipendium der ÖKG). The Austrian Science Fund supports S.F. (P27166-B23), A.P. (I3165, P29328-B26) and F.M. (P27893, P31727). S.S., J.V., F.M. and S.L.H. acknowledge support from the BioTechMed–Graz. G.K. is supported by the Ligue contre le Cancer (équipe labellisée); Association pour la recherche sur le cancer (ARC); Association Ruban Rose, Cancéropôle Ile-de-France; Chancellerie des universités de Paris (Legs Poix), Fondation pour la Recherche Médicale (FRM); Institut National du Cancer (INCa); Inserm (HTE); Inserm Transfert; Institut Universitaire de France; LeDucq Foundation; the LabEx Immuno-Oncology (ANR-18-IDEX-0001); the SIRIC Stratified Oncology Cell DNA Repair and Tumor Immune Elimination (SOCRATE); the SIRIC Cancer Research and Personalized Medicine (CARPEM). J.A.C. acknowledges funding from the Ministerio de Ciencia e Innovación (MCIN) through grant BIO2017-83640-P (AEI/FEDER, UE) and the Comunidad de Madrid (consortium Tec4Bio-CM, S2018/NMT-4443, FEDER). A.S. acknowledges support from BioPersMed Graz. S.K. receives funding from the Austrian Research Promotion Agency FFG (VASCage; Nr. 868624). The Bruneck Study was supported by the Pustertaler Verein zur Prävention von Herz-und Hirngefäßerkrankungen, Gesundheitsbezirk Bruneck, and the Assessorat für Gesundheit, Province of Bolzano, Italy.

Data and Material availability

All data associated with this study are in the paper or Supplementary Materials. The RNA-seq data are accessible on the NCBI GEO database under the accession number GSE163665.

References

1. Vasan RS, Xanthakis V, Lyass A, Andersson C, Tsao C, Cheng S, Aragam J, Benjamin EJ, Larson MG. Epidemiology of Left Ventricular Systolic Dysfunction and Heart Failure in the Framingham Study: An Echocardiographic Study Over 3 Decades. *JACC Cardiovasc Imaging*. 2018; 11 :1–11. [PubMed: 28917679]
2. Dunlay SM, Roger VL, Redfield MM. Epidemiology of heart failure with preserved ejection fraction. *Nat Rev Cardiol*. 2017; 14 :591–602. [PubMed: 28492288]
3. Fonarow GC, Stough WG, Abraham WT, Albert NM, Gheorghiane M, Greenberg BH, O'Connor CM, Sun JL, Yancy CW, Young JB. OPTIMIZE-HF Investigators and Hospitals, Characteristics, treatments, and outcomes of patients with preserved systolic function hospitalized for heart failure: a report from the OPTIMIZE-HF Registry. *J Am Coll Cardiol*. 2007; 50 :768–777. [PubMed: 17707182]
4. Lourenço AP, Leite-Moreira AF, Balligand J-L, Bauersachs J, Dawson D, de Boer RA, de Windt LJ, Falcão-Pires I, Fontes-Carvalho R, Franz S, Giacca M, et al. An integrative translational approach to study heart failure with preserved ejection fraction: a position paper from the Working Group on Myocardial Function of the European Society of Cardiology. *Eur J Heart Fail*. 2018; 20 :216–227. [PubMed: 29148148]
5. Paulus WJ, Tschöpe C. A novel paradigm for heart failure with preserved ejection fraction: comorbidities drive myocardial dysfunction and remodeling through coronary microvascular endothelial inflammation. *J Am Coll Cardiol*. 2013; 62 :263–271. [PubMed: 23684677]
6. Schiattarella GG, Altamirano F, Tong D, French KM, Villalobos E, Kim SY, Luo X, Jiang N, May HI, Wang ZV, Hill TM, et al. Nitrosative stress drives heart failure with preserved ejection fraction. *Nature*. 2019; 568 :351–356. [PubMed: 30971818]
7. Dewan P, Rørth R, Raparelli V, Campbell RT, Shen L, Jhund PS, Petrie MC, Anand IS, Carson PE, Desai AS, Granger CB, et al. Sex-Related Differences in Heart Failure With Preserved Ejection Fraction. *Circ Heart Fail*. 2019; 12 e006539 [PubMed: 31813280]
8. Solomon SD, McMurray JJV, Anand IS, Ge J, Lam CSP, Maggioni AP, Martinez F, Packer M, Pfeffer MA, Pieske B, Redfield MM, et al. PARAGON-HF Investigators and Committees, Angiotensin-Nephrilysin Inhibition in Heart Failure with Preserved Ejection Fraction. *N Engl J Med*. 2019; 381 :1609–1620. [PubMed: 31475794]
9. Di Francesco A, Di Germanio C, Bernier M, de Cabo R. A time to fast. *Science*. 2018; 362 :770–775. [PubMed: 30442801]
10. Kitzman DW, Brubaker P, Morgan T, Haykowsky M, Hundley G, Kraus WE, Eggebeen J, Nicklas BJ. Effect of Caloric Restriction or Aerobic Exercise Training on Peak Oxygen Consumption and

- Quality of Life in Obese Older Patients With Heart Failure With Preserved Ejection Fraction: A Randomized Clinical Trial. *JAMA*. 2016; 315 :36–46. [PubMed: 26746456]
11. Madeo F, Carmona-Gutierrez D, Hofer SJ, Kroemer G. Caloric Restriction Mimetics against Age-Associated Disease: Targets, Mechanisms, and Therapeutic Potential. *Cell Metab*. 2019; 29 :592–610. [PubMed: 30840912]
 12. Rajman L, Chwalek K, Sinclair DA. Therapeutic Potential of NAD-Boosting Molecules: The In Vivo Evidence. *Cell Metab*. 2018; 27 :529–547. [PubMed: 29514064]
 13. Mitchell SJ, Bernier M, Aon MA, Cortassa S, Kim EY, Fang EF, Palacios HH, Ali A, Navas-Enamorado I, Di Francesco A, Kaiser TA, et al. Nicotinamide Improves Aspects of Healthspan, but Not Lifespan, in Mice. *Cell Metab*. 2018; 27 :667–676. e4 [PubMed: 29514072]
 14. Summer G, Kuhn AR, Munts C, Miranda-Silva D, Leite-Moreira AF, Lourenço AP, Heymans S, Falcão-Pires I, van Bilsen M. A directed network analysis of the cardiome identifies molecular pathways contributing to the development of HFpEF. *J Mol Cell Cardiol*. 2020; 144 :66–75. [PubMed: 32422321]
 15. Hamdani N, Franssen C, Lourenço A, Falcão-Pires I, Fontoura D, Leite S, Plettig L, López B, Ottenheijm CA, Becher PM, González A, et al. Myocardial titin hypophosphorylation importantly contributes to heart failure with preserved ejection fraction in a rat metabolic risk model. *Circ Heart Fail*. 2013; 6 :1239–1249. [PubMed: 24014826]
 16. Leite S, Oliveira-Pinto J, Tavares-Silva M, Abdellatif M, Fontoura D, Falcão-Pires I, Leite-Moreira AF, Lourenço AP. Echocardiography and invasive hemodynamics during stress testing for diagnosis of heart failure with preserved ejection fraction: an experimental study. *Am J Physiol Heart Circ Physiol*. 2015; 308 :H1556–1563. [PubMed: 25862827]
 17. Mahmood M, Pal N, Rayner J, Holloway C, Raman B, Dass S, Levelt E, Ariga R, Ferreira V, Banerjee R, Schneider JE, et al. The interplay between metabolic alterations, diastolic strain rate and exercise capacity in mild heart failure with preserved ejection fraction: a cardiovascular magnetic resonance study. *J Cardiovasc Magn Reson*. 2018; 20 :88. [PubMed: 30580760]
 18. Menzies KJ, Zhang H, Katsyuba E, Auwerx J. Protein acetylation in metabolism – metabolites and cofactors. *Nat Rev Endocrinol*. 2016; 12 :43–60. [PubMed: 26503676]
 19. Hong S, Moreno-Navarrete JM, Wei X, Kikukawa Y, Tzamelis I, Prasad D, Lee Y, Asara JM, Fernandez-Real JM, Maratos-Flier E, Pissios P. Nicotinamide N-methyltransferase regulates hepatic nutrient metabolism through Sirt1 protein stabilization. *Nat Med*. 2015; 21 :887–894. [PubMed: 26168293]
 20. Eisner DA, Caldwell JL, Trafford AW, Hutchings DC. The Control of Diastolic Calcium in the Heart: Basic Mechanisms and Functional Implications. *Circ Res*. 2020; 126 :395–412. [PubMed: 31999537]
 21. Gorski PA, Jang SP, Jeong D, Lee A, Lee P, Oh JG, Chepurko V, Yang DK, Kwak TH, Eom SH, Park Z-Y, et al. Role of SIRT1 in Modulating Acetylation of the Sarco-Endoplasmic Reticulum Ca²⁺-ATPase in Heart Failure. *Circ Res*. 2019; 124 :e63–e80. [PubMed: 30786847]
 22. Koser F, Loescher C, Linke WA. Posttranslational modifications of titin from cardiac muscle: how, where, and what for? *FEBS J*. 2019; 286 :2240–2260. [PubMed: 30989819]
 23. Klotz S, Hay I, Zhang G, Maurer M, Wang J, Burkhoff D. Development of heart failure in chronic hypertensive Dahl rats: focus on heart failure with preserved ejection fraction. *Hypertension*. 2006; 47 :901–911. [PubMed: 16585423]
 24. Eisenberg T, Abdellatif M, Schroeder S, Primessnig U, Stekovic S, Pendl T, Harger A, Schipke J, Zimmermann A, Schmidt A, Tong M, et al. Cardioprotection and lifespan extension by the natural polyamine spermidine. *Nat Med*. 2016; 22 :1428–1438. [PubMed: 27841876]
 25. Chiao YA, Rabinovitch PS. The Aging Heart. *Cold Spring Harb Perspect Med*. 2015; 5 a025148 [PubMed: 26328932]
 26. Institute of Medicine (US) Standing Committee on the Scientific Evaluation of Dietary Reference Intakes and its Panel on Folate, Other B Vitamins, and Choline. Dietary Reference Intakes for Thiamin Riboflavin Niacin Vitamin B6 Folate Vitamin B12 Pantothenic Acid Biotin and Choline. National Academies Press (US); Washington (DC): 1998. <http://www.ncbi.nlm.nih.gov/books/NBK114310/>

27. Kiechl S, Willeit J. In a Nutshell: Findings from the Bruneck Study. *Gerontology*. 2019; 65 :9–19. [PubMed: 30179866]
28. Pieske B, Tschöpe C, de Boer RA, Fraser AG, Anker SD, Donal E, Edelmann F, Fu M, Guazzi M, Lam CSP, Lancellotti P, et al. How to diagnose heart failure with preserved ejection fraction: the HFA-PEFF diagnostic algorithm: a consensus recommendation from the Heart Failure Association (HFA) of the European Society of Cardiology (ESC). *European Heart Journal*. 2019; 40 :3297–3317. [PubMed: 31504452]
29. Reddy YNV, Carter RE, Obokata M, Redfield MM, Borlaug BA. A Simple, Evidence-Based Approach to Help Guide Diagnosis of Heart Failure With Preserved Ejection Fraction. *Circulation*. 2018; 138 :861–870. [PubMed: 29792299]
30. Diguët N, Trammell SAJ, Tannous C, Deloux R, Piquereau J, Mougénot N, Gouge A, Gressette M, Manoury B, Blanc J, Breton M, et al. Nicotinamide Riboside Preserves Cardiac Function in a Mouse Model of Dilated Cardiomyopathy. *Circulation*. 2018; 137 :2256–2273. [PubMed: 29217642]
31. Leite S, Rodrigues S, Tavares-Silva M, Oliveira-Pinto J, Alaa M, Abdellatif M, Fontoura D, Falcão-Pires I, Gillebert TC, Leite-Moreira AF, Lourenço AP, et al. Afterload-induced diastolic dysfunction contributes to high filling pressures in experimental heart failure with preserved ejection fraction. *Am J Physiol Heart Circ Physiol*. 2015; 309 :H1648–1654. [PubMed: 26408538]
32. Jeong MY, Lin YH, Wennersten SA, Demos-Davies KM, Cavasin MA, Mahaffey JH, Monzani V, Saripalli C, Mascagni P, Reece TB, Ambardekar AV, et al. Histone deacetylase activity governs diastolic dysfunction through a nongenomic mechanism. *Sci Transl Med*. 2018; 10 doi: 10.1126/scitranslmed.aao0144
33. Wallner M, Eaton DM, Berretta RM, Liesinger L, Schittmayer M, Gindlhuber J, Wu J, Jeong MY, Lin YH, Borghetti G, Baker ST, et al. HDAC inhibition improves cardiopulmonary function in a feline model of diastolic dysfunction. *Sci Transl Med*. 2020; 12 eaay7205 [PubMed: 31915304]
34. Zhou B, Wang DD-H, Qiu Y, Airhart S, Liu Y, Stempien-Otero A, O'Brien KD, Tian R. Boosting NAD level suppresses inflammatory activation of PBMCs in heart failure. *J Clin Invest*. 2020; doi: 10.1172/JCI138538
35. Hong G, Zheng D, Zhang L, Ni R, Wang G, Fan G-C, Lu Z, Peng T. Administration of nicotinamide riboside prevents oxidative stress and organ injury in sepsis. *Free Radic Biol Med*. 2018; 123 :125–137. [PubMed: 29803807]
36. Horton JL, Martin OJ, Lai L, Riley NM, Richards AL, Vega RB, Leone TC, Pagliarini DJ, Muoio DM, Bedi KC, Margulies KB, et al. Mitochondrial protein hyperacetylation in the failing heart. *JCI Insight*. 2016; 2 doi: 10.1172/jci.insight.84897
37. Lee CF, Chavez JD, Garcia-Menendez L, Choi Y, Roe ND, Chiao YA, Edgar JS, Goo YA, Goodlett DR, Bruce JE, Tian R, et al. Normalization of NAD⁺ Redox Balance as a Therapy for Heart Failure. *Circulation*. 2016; 134 :883–894. [PubMed: 27489254]
38. Liu L, Su X, Quinn WJ, Hui S, Krukenberg K, Frederick DW, Redpath P, Zhan L, Chellappa K, White E, Migaud M, et al. Quantitative Analysis of NAD Synthesis-Breakdown Fluxes. *Cell Metab*. 2018; 27 :1067–1080. e5 [PubMed: 29685734]
39. McReynolds, Melanie; Chellappa, Karthikeyani; Chiles, Eric; Jankowski, Connor; Shen, Yishui; Chen, Li; Descamps, Helene; Mukherjee, Sarmistha; Bhat, Yashaswini; Chu, Qingwei; Botolin, Paul; , et al. NAD⁺ flux is maintained in aged mice. PREPRINT (Version 1) available at Research Square. 2020 Oct 9. doi: 10.21203/rs.3.rs-86538/v1
40. Vignier N, Chatzifrangkeskou M, Morales Rodriguez B, Mericskay M, Mougénot N, Wahbi K, Bonne G, Muchir A. Rescue of biosynthesis of nicotinamide adenine dinucleotide protects the heart in cardiomyopathy caused by lamin A/C gene mutation. *Hum Mol Genet*. 2018; 27 :3870–3880. [PubMed: 30053027]
41. Poyan Mehr A, Tran MT, Ralto KM, Leaf DE, Washco V, Messmer J, Lerner A, Kher A, Kim SH, Khoury CC, Herzig SJ, et al. De novo NAD⁺ biosynthetic impairment in acute kidney injury in humans. *Nat Med*. 2018; 24 :1351–1359. [PubMed: 30127395]
42. Abdellatif M, Leite S, Alaa M, Oliveira-Pinto J, Tavares-Silva M, Fontoura D, Falcão-Pires I, Leite-Moreira AF, Lourenço AP. Spectral transfer function analysis of respiratory hemodynamic fluctuations predicts end-diastolic stiffness in preserved ejection fraction heart failure. *Am J Physiol Heart Circ Physiol*. 2016; 310 :H4–13. [PubMed: 26475584]

43. Willett W, Stampfer MJ. Total energy intake: implications for epidemiologic analyses. *Am J Epidemiol.* 1986; 124 :17–27. [PubMed: 3521261]
44. Sedej S, Schmidt A, Denegri M, Walther S, Matovina M, Arnstein G, Gutschi E-M, Windhager I, Ljubojević S, Negri S, Heinzl FR, et al. Subclinical abnormalities in sarcoplasmic reticulum Ca(2+) release promote eccentric myocardial remodeling and pump failure death in response to pressure overload. *J Am Coll Cardiol.* 2014; 63 :1569–1579. [PubMed: 24315909]
45. Hamdani N, Krysiak J, Kreusser MM, Neef S, Dos Remedios CG, Maier LS, Kruger M, Backs J, Linke WA. Crucial role for Ca2(+)/calmodulin-dependent protein kinase-II in regulating diastolic stress of normal and failing hearts via titin phosphorylation. *Circ Res.* 2013; 112 :664–674. [PubMed: 23283722]
46. Mina AI, LeClair RA, LeClair KB, Cohen DE, Lantier L, Banks AS. CalR: A Web-Based Analysis Tool for Indirect Calorimetry Experiments. *CellMetab.* 2018; 28 :656–666. e1
47. Tschöp MH, Speakman JR, Arch JRS, Auwerx J, Brüning JC, Chan L, Eckel RH, Farese RV, Galgani JE, Hambly C, Herman MA, et al. A guide to analysis of mouse energy metabolism. *Nat Methods.* 2011; 9 :57–63. [PubMed: 22205519]
48. Herrero-Galán E, Domínguez F, Martínez-Martín I, Sánchez-González C, Vicente N, Lalaguna L, Bonzón-Kulichenko E, Calvo E, González-López E, Cobo-Marcos M, Bornstein B, et al. Conserved cysteines in titin sustain the mechanical function of cardiomyocytes. *bioRxiv.* 2020 Sep 05. 282913
49. Schipke J, Brandenberger C, Rajces A, Manninger M, Alogna A, Post H, Mühlfeld C. Assessment of cardiac fibrosis: a morphometric method comparison for collagen quantification. *J Appl Physiol.* 2017; 122 :1019–1030. [PubMed: 28126909]
50. Briguet A, Courdier-Fruh I, Foster M, Meier T, Magyar JP. Histological parameters for the quantitative assessment of muscular dystrophy in the mdx-mouse. *Neuromuscul Disord.* 2004; 14 :675–682. [PubMed: 15351425]
51. Viltard M, Durand S, Pérez-Lanzón M, Aprahamian F, Lefevre D, Leroy C, Madeo F, Kroemer G, Friedlander G. The metabolomic signature of extreme longevity: naked mole rats versus mice. *Aging (Albany NY).* 2019; 11 :4783–4800. [PubMed: 31346149]
52. Chong J, Wishart DS, Xia J. Using MetaboAnalyst 4.0 for Comprehensive and Integrative Metabolomics Data Analysis. *Curr Protoc Bioinformatics.* 2019; 68 :e86. [PubMed: 31756036]
53. Prieto C, Barrios D. RaNA-Seq: Interactive RNA-Seq analysis from FASTQ files to functional analysis. *Bioinformatics.* 2019; doi: 10.1093/bioinformatics/btz854
54. Subramanian A, Tamayo P, Mootha VK, Mukherjee S, Ebert BL, Gillette MA, Paulovich A, Pomeroy SL, Golub TR, Lander ES, Mesirov JP. Gene set enrichment analysis: a knowledge-based approach for interpreting genome-wide expression profiles. *Proc Natl Acad Sci USA.* 2005; 102 :15545–15550. [PubMed: 16199517]
55. Rappsilber J, Ishihama Y, Mann M. Stop and go extraction tips for matrix-assisted laser desorption/ionization, nanoelectrospray, and LC/MS sample pretreatment in proteomics. *Anal Chem.* 2003; 75 :663–670. [PubMed: 12585499]
56. Nolte H, Hölper S, Selbach M, Braun T, Krüger M. Assessment of serum protein dynamics by native SILAC flooding (SILflood). *Anal Chem.* 2014; 86 :11033–11037. [PubMed: 25347402]
57. Cox J, Neuhauser N, Michalski A, Scheltema RA, Olsen JV, Mann M. Andromeda: a peptide search engine integrated into the MaxQuant environment. *J Proteome Res.* 2011; 10 :1794–1805. [PubMed: 21254760]
58. Nolte H, MacVicar TD, Tellkamp F, Krüger M. Instant Clue: A Software Suite for Interactive Data Visualization and Analysis. *Sci Rep.* 2018; 8 :12648 [PubMed: 30140043]
59. Vasques-Nóvoa F, Laundos TL, Cerqueira RJ, Quina-Rodrigues C, Soares-Dos-Reis R, Baganha F, Ribeiro S, Mendonça L, Gonçalves F, Reguenga C, Verhesen W, et al. MicroRNA-155 Amplifies Nitric Oxide/cGMP Signaling and Impairs Vascular Angiotensin II Reactivity in Septic Shock. *Crit Care Med.* 2018; 46 :e945–e954. [PubMed: 29979224]
60. Lara TM. Skeletal Muscle Phosphocreatine Depletion Depresses Myocellular Energy Status During Sepsis. *Arch Surg.* 1998; 133 :1316. [PubMed: 9865649]
61. Ingwall, JS. *ATP and the Heart.* Springer; US Boston, MA: 2002.

62. Kiechl S, Lorenz E, Reindl M, Wiedermann CJ, Oberhollenzer F, Bonora E, Willeit J, Schwartz DA. Toll-like receptor 4 polymorphisms and atherogenesis. *N Engl J Med.* 2002; 347 :185–192. [PubMed: 12124407]
63. Kiechl S, Schett G, Schwaiger J, Seppi K, Eder P, Egger G, Santer P, Mayr A, Xu Q, Willeit J. Soluble receptor activator of nuclear factor-kappa B ligand and risk for cardiovascular disease. *Circulation.* 2007; 116 :385–391. [PubMed: 17620507]
64. Willett WC, Sampson L, Stampfer MJ, Rosner B, Bain C, Witschi J, Hennekens CH, Speizer FE. Reproducibility and validity of a semiquantitative food frequency questionnaire. *Am J Epidemiol.* 1985; 122 :51–65. [PubMed: 4014201]

One Sentence Summary

The NAD⁺ precursor nicotinamide improves diastolic dysfunction caused by aging, hypertension or metabolic syndrome in rodents.

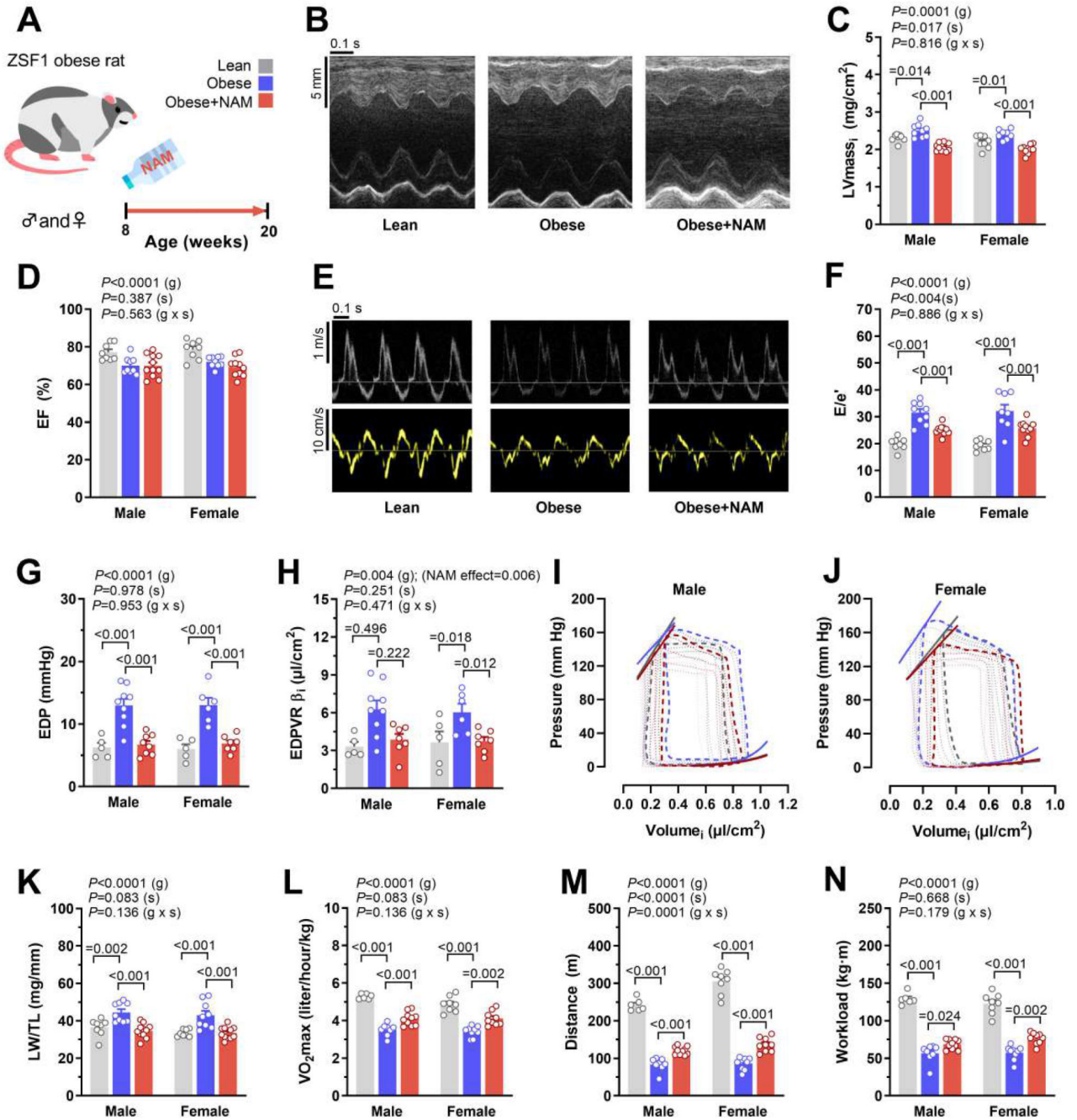


Fig. 1. Oral supplementation of NAM improves diastolic dysfunction in ZSF1 obese rats. (A) Schematic overview of nicotinamide (NAM) feeding protocol to male and female ZSF1 obese rats with cardiometabolic syndrome and HFpEF. NAM (40 mM) was added to the drinking water starting at the age of 8 weeks and after 3 months cardiac parameters were assessed. (B) Representative echocardiography-derived M-mode tracings, (C) left ventricular mass indexed to body surface area (LVmassi), (D) ejection fraction (EF), (E) representative pulsed-wave Doppler (*top*) and tissue Doppler (*bottom*) tracings, and (F) ratio of peak early Doppler transmitral flow velocity (*E*) to myocardial tissue Doppler

velocity (e^{\dagger}), ($n=8/9/10$ and $8/9/11$ rats for lean/obese/obese+NAM in males and females, respectively). **(G)** Invasive hemodynamic assessment of left ventricular end-diastolic pressure (EDP), **(H)** myocardial stiffness constant (indexed end-diastolic pressure volume exponential relationship coefficient β . EDPVR β_i), **(I and J)** end-systolic and end-diastolic pressure volume relationships generated by inferior vena cava occlusions with corresponding pressure-volume loops in **(I)** male and **(J)** female ZSF1 rats, ($n=5/9/8$ and $5/6/7$ rats for lean/obese/obese+NAM in males and females, respectively). **(K)** Lung weight normalized to tibia length (LW/TL), ($n=8/9/11$ rats for lean/obese/obese+NAM in either sex). **(L)** Maximal oxygen consumption (VO^2_{max}), **(M)** running distance, and **(N)** workload in ZSF1 rats during exercise exhaustion testing, ($n=6/8/10$ and $8/9/9$ rats for lean/obese/obese+NAM in males and females, respectively). All results were generated from 2 independent cohorts. Indicated P values on top of panels (C and D, F to H, and K to N) represent factor comparisons by a linear mixed model including sex (s) and group (g) as fixed factors and the cohort as a random factor; following comparisons between different groups within the respective sex are indicated by Bonferroni post-hoc test. EDPVR α_i was included in the model as a covariate in (F). Bars and error bars show means and SEM, respectively, with individual data points superimposed.

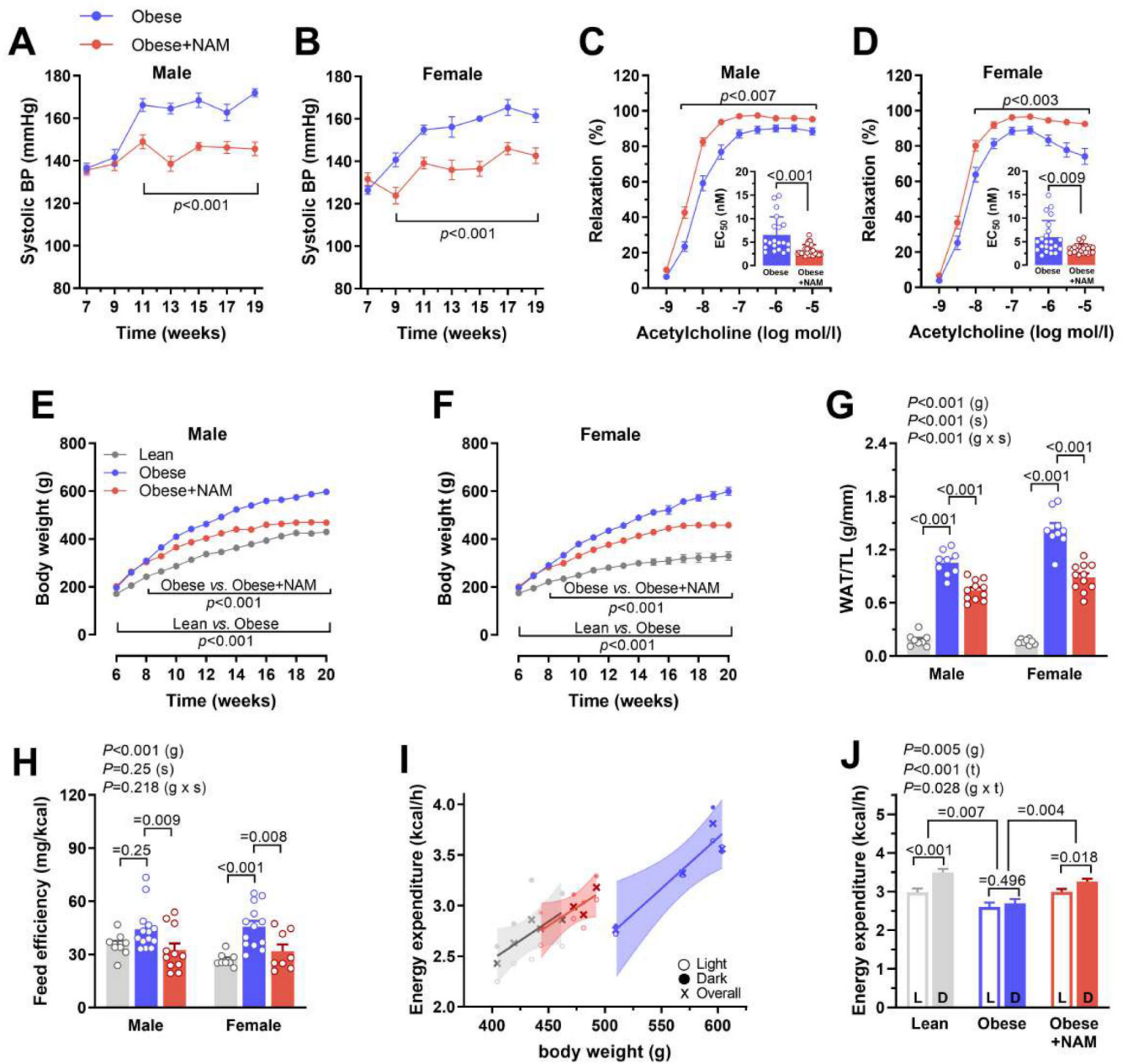


Fig. 2. NAM ameliorates blood pressure control and adiposity in ZSF1 obese rats.

(A and B) Systolic arterial blood pressure, non-invasively measured by the tail-cuff method, in (A) male and (B) female ZSF1 obese rats treated or not with nicotinamide (NAM) starting from 8 weeks. ($n=10/11$ and $9/11$ rats in obese/obese+NAM in males and females, respectively). (C and D) Acetylcholine-induced vasodilation measured *ex vivo* in the aortic rings of (C) male and (D) female rats; Inset graphs denote corresponding EC₅₀ of single rings, ($n=20/24$ and $22/23$ rings obtained from 4 obese/obese+NAM in males and females, respectively). (E and F) Body weight gain of (E) male and (F) female ZSF1 obese rats and their lean controls, ($n=8/9/11$ and $10/9/11$ rats in lean/obese/obese+NAM for males and females, respectively). (G) Visceral white adipose tissue (WAT) normalized to tibia length

(TL), ($n=8/9/11$ rats for lean/obese/obese+NAM in either gender). **(H)** Feeding efficiency (body weight gain per consumed *kcal* energy) measured during the first 2-3 weeks of treatment before the obvious body weight difference thereafter, ($n=8/14/11$ and $8/13/8$ rats in lean/obese/obese+NAM for males and females, respectively). **(I)** Energy expenditure (shown as a function of body weight) evaluated by indirect calorimetry, and **(J)** estimated energy expenditure (during dark and light cycles of the day) at a hypothetical equal body weight (490.6 g) in all groups as derived from corresponding analysis of covariance (ANCOVA), ($n=4$ male rats per group). L, light; D, dark. All results except in I and J were generated from 2 independent cohorts. (A to F) *P* values were calculated by two-way repeated measures ANOVA, followed by Bonferroni-corrected pairwise comparisons; (C and D) EC_{50} were compared by Mann-Whitney test. (G and H) Indicated *P* values on top of panels represent factor comparisons by a linear mixed model including sex (s) and group (g) as fixed factors and the cohort as a random factor, and following comparisons between different groups within respective sex are indicated by Bonferroni post-hoc tests. (J) Factorial ANCOVA was used including group (g) and time of the day (t; light vs. dark 12h cycles) as fixed factors and body weight as a covariate, followed by Bonferroni-corrected pairwise comparisons. Circles/Bars and error bars show means and SEM, respectively, with individual data points superimposed, except for (J) where the means and SEM were derived from ANCOVA and corresponding individual data points are shown in (I).

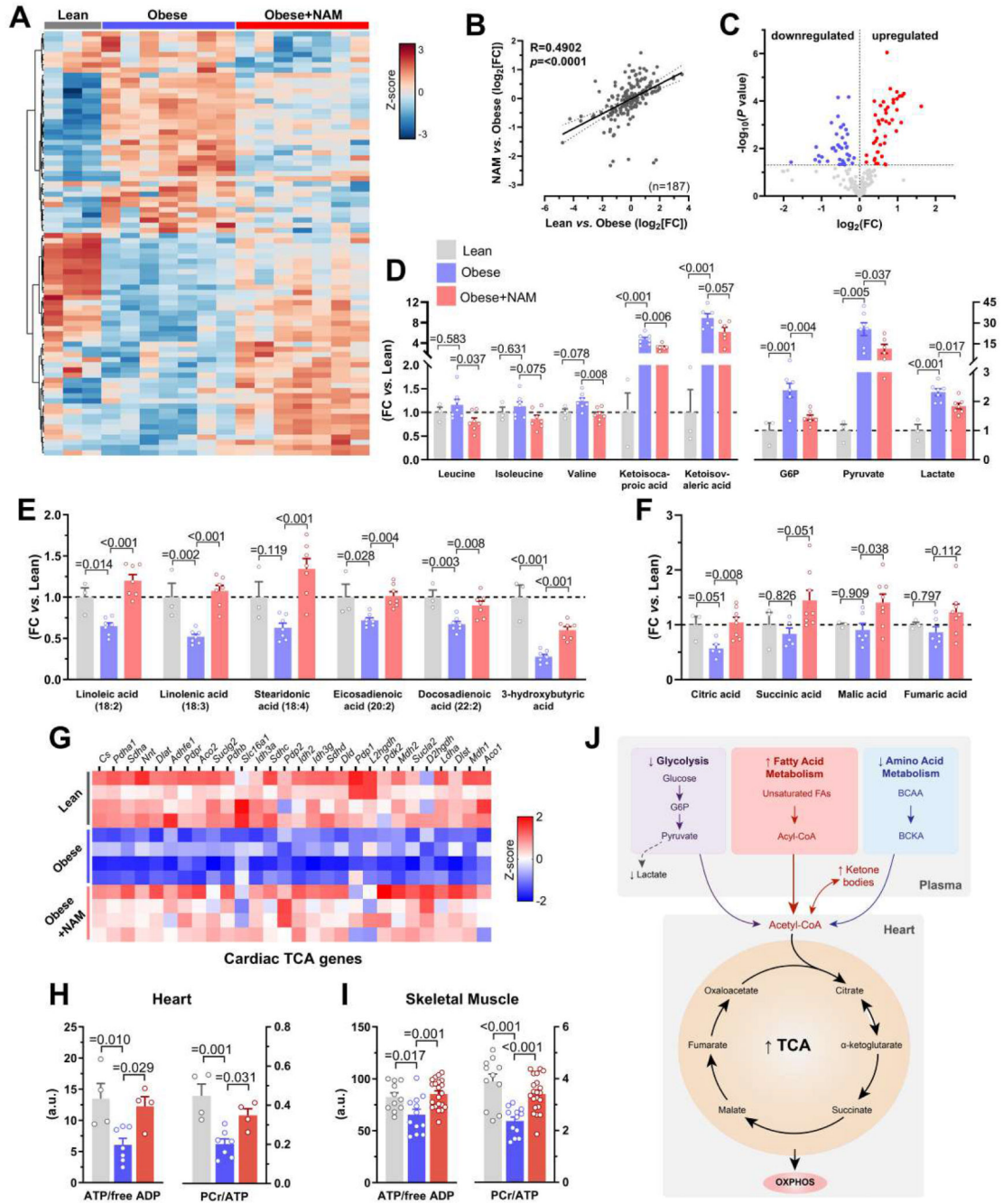


Fig. 3. NAM-mediated metabolic reprogramming improves energy homeostasis in HFpEF. (A) Heatmap depicting relative abundance of significantly differentiated metabolites by nicotinamide (NAM) in the plasma of 12-week-old ZSF1 obese rats (4 weeks of NAM treatment) that were fasted for 6 hours, ($n=3/7/7$ rats in lean/obese/obese+NAM). (B) Correlation of NAM-induced metabolomic changes vs. the difference between ZSF1 lean and obese controls ($\text{Log}_2[\text{fold-change, FC}]$). (C) Volcano plot showing up- and down-regulated metabolites of NAM-treated vs. control ZSF1 obese rats. (D and E) Relative difference in selected circulating metabolites related to (D) branched-chain amino acids

metabolism (*left*) and glycolysis (*right*), as well as (E) lipolysis and ketogenesis (shown are polyunsaturated fatty acids and ketone bodies, please see also fig. S7 for other related metabolites), ($n=3/7/7$ rats in lean/obese/obese+NAM). (F) Relative abundance of tricarboxylic acid cycle (TCA) metabolites in left ventricular tissue of 20-week-old NAM-treated ZSF1 obese rats compared to age-matched obese and lean controls, ($n=3/6/8$ rats in lean/obese/obese+NAM). (G) Heatmaps of cardiac transcripts showing the expression (red=high, blue=low) of differentially regulated genes involved in TCA cycle in ZSF1 lean, obese and NAM-treated obese rats, ($n=4$ rats per group). (H and I) High-energy phosphate compounds in (H) the heart and (I) skeletal muscle (*i.e.*, gastrocnemius) of ZSF1 rats, ($n=4/7/4$ and $11/12/21$ rats in lean/obese/obese+NAM for heart and skeletal muscle, respectively). PCr, phosphocreatine; ATP, adenosine triphosphate; ADP, adenosine diphosphate. (J) Schematic representation of affected metabolic pathways by NAM supplementation. *Abbreviations*: BCAA, branched-chain amino acids; BCKA, branched-chain keto acids; G6P, glucose-6-phosphate. *P* values were calculated by (B) Pearson correlation, (C) Welch t-test or (D to F and H to I) ANOVA with Dunnett's post-hoc test. Bars and error bars show means and SEM, respectively, with individual data points superimposed.

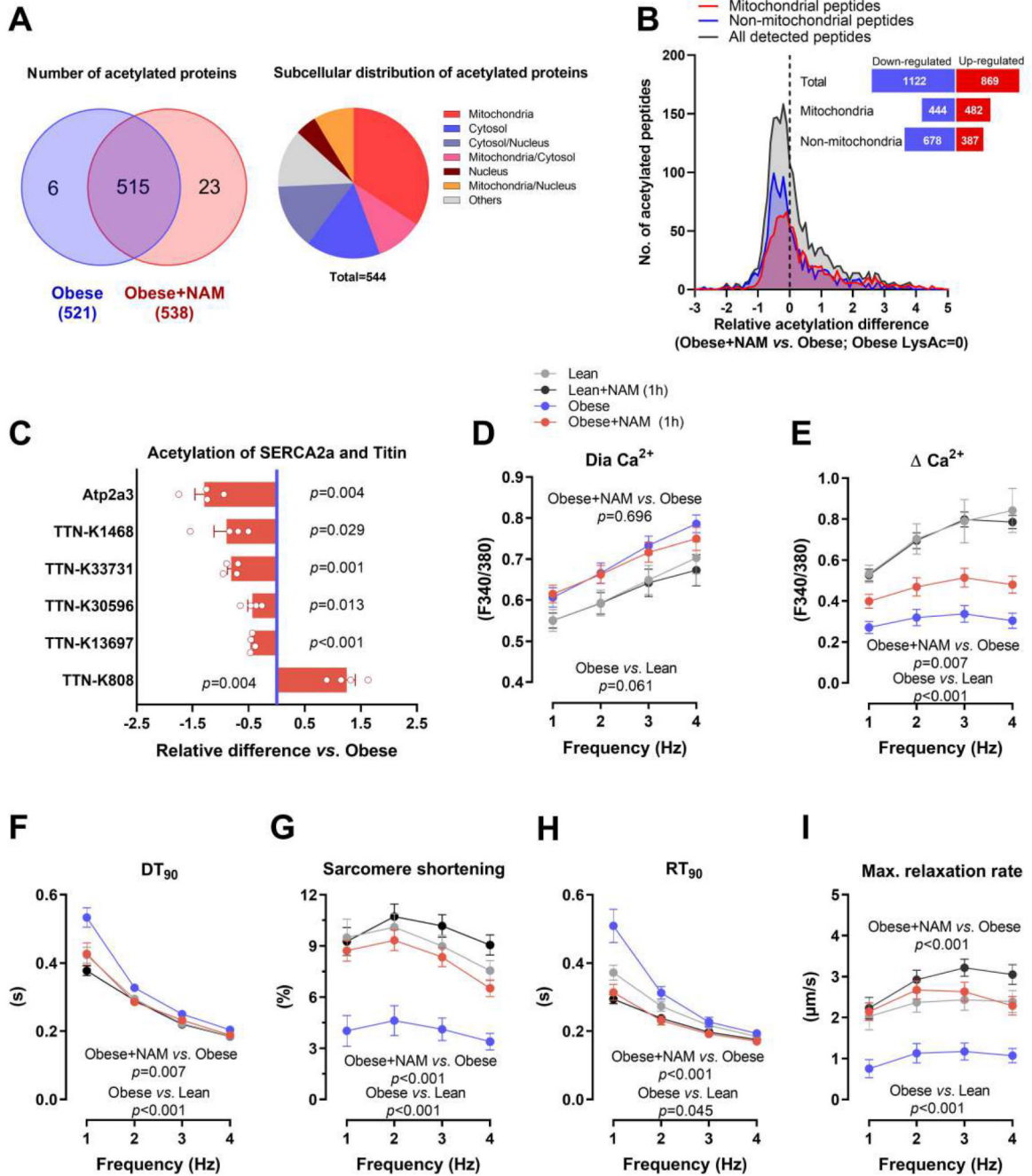


Fig. 4. SERCA2a deacetylation contributes to improved diastolic function by NAM.

(A) Venn diagram (*left*) showing the overlap of detected acetylated proteins in the hearts of control and NAM-treated 20-week-old male ZSF1 obese rats, along with their subcellular localization in a pie chart (*right*). (B) Distribution of NAM-induced changes in acetylation of cardiac peptides (mitochondrial and non-mitochondrial); the dashed line denotes acetylation in control ZSF1 obese rats. The inset figure denotes the sum of peptides with up- or down-regulated acetylation. (C) Relative signal intensity difference of significantly regulated acetylation sites in titin and SERCA2a (Atp2a3). Note that negative values

indicate deacetylation and positive ones indicate acetylation, ($n=4$ obese+NAM compared to the average of 3 obese). **(D)** Diastolic (Dia) calcium and **(E)** changes in calcium transient amplitude as indicated by Fura-2/AM ratio (340:380 nm), **(F)** time to 90% decay (DT_{90}), along with **(G)** simultaneously measured sarcomere shortening, **(H)** time to 90% relaxation (RT_{90}) and **(I)** maximal relaxation rate of electrically-paced adult ZSF1 obese and lean cardiomyocytes that were pre-incubated or not with NAM (100 μ M) for one hour, ($n=18/20/18/23$ cardiomyocytes in lean/lean+NAM/obese/obese+NAM isolated from 4 lean and 4 obese ZSF1 rats at the age of 20 weeks). *P* values were calculated by (C) one-sample t-test or (D to I) two-way repeated measures ANOVA. Bars/circles and error bars show means and SEM, respectively, with individual data points superimposed.

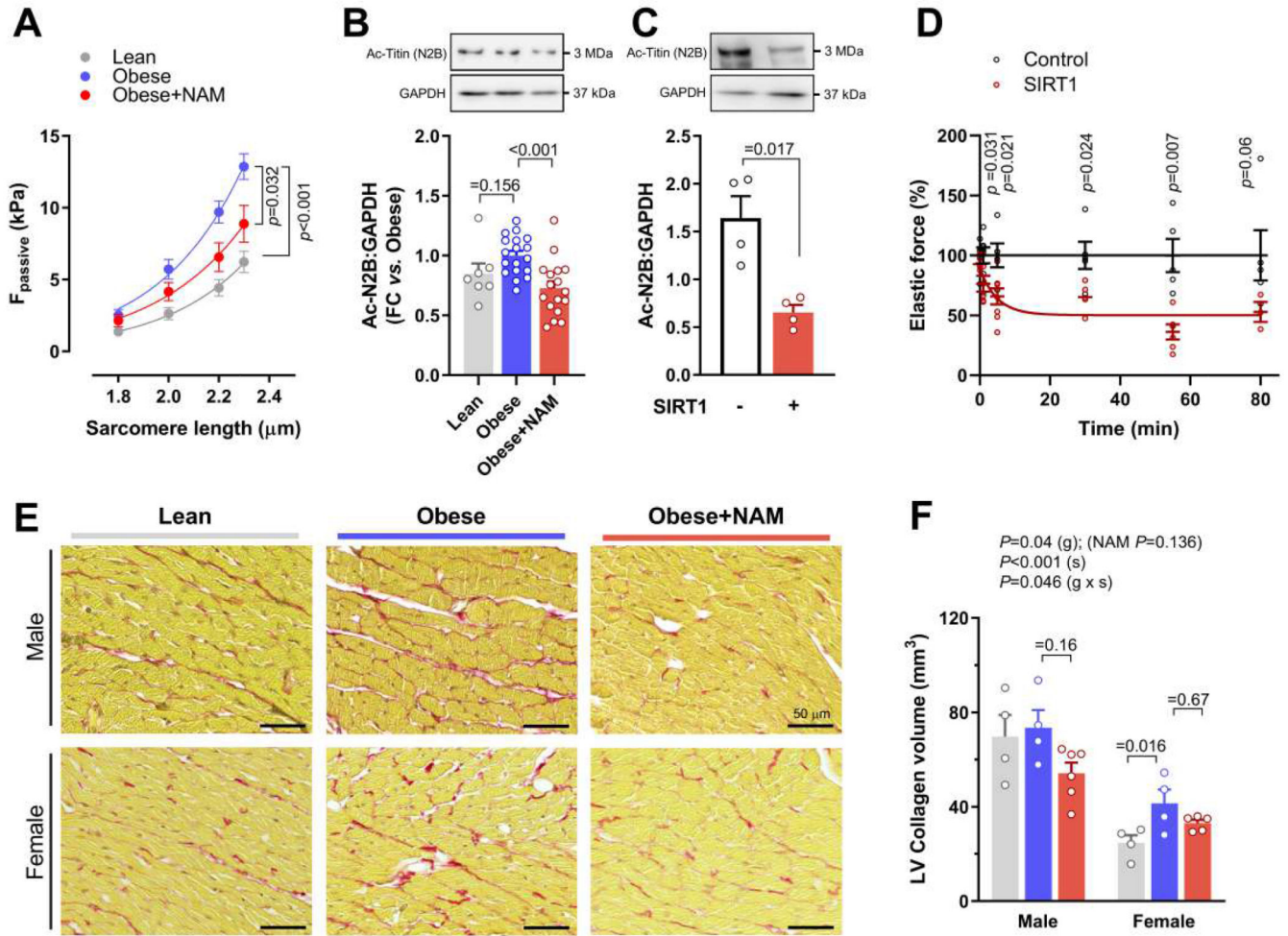


Fig. 5. Titin deacetylation is sufficient to improve cardiomyocyte passive stiffness.

(A) The relationship between passive force (F_{passive}) and sarcomere length, indicative of passive stiffness, in skinned cardiomyocytes isolated from 20-week-old ZSF1 lean and obese rats treated or not with nicotinamide (NAM). Exponential curves are fitted to the group average ($n=18/16/21$ cardiomyocytes in lean/obese/obese+NAM isolated from 4/3/4 rats, respectively). (B and C) Representative Western blot (top) and quantification (bottom) of (B) cardiac titin acetylation (normalized to GAPDH) in 20-week-old ZSF1 rats, ($n=7/18/17$ rats in lean/obese/obese+NAM), (C) In vitro deacetylation of titin N2B isoform in skinned cardiomyocytes from healthy 20-week-old Wistar-Kyoto rats. Cells were incubated with recombinant SIRT1 for 2 hours at 30°C. Representative Western blot (top panels) probed with acetylated-lysine-specific antibodies for detection of total N2B acetylation; GAPDH antibody was used as a loading control. Lower panel shows quantification of titin-N2B acetylation normalized to GAPDH ($N=4$ rats per group). (D) Relative change in passive force of isolated skinned cardiomyocytes upon deacetylation with recombinant SIRT1 compared to control cells force that is measured in the same buffer but without SIRT1, ($n=3-8$ cardiomyocytes per condition and per time point). Data points are fitted using a one-phase decay curve fit. (E) Representative micrographs and (F)

quantification of left ventricular (LV) fibrotic remodelling due to collagen accumulation, as evaluated by picrosirius red staining in 20-week-old male and female ZSF1 rats, ($n=4/4/6$ and $4/4/5$ for lean/obese/obese+NAM in males and females, respectively). *P* values were calculated by (A) two-way repeated measures ANOVA with Dunnett's post-hoc test, (B) ANOVA with Dunnett's post-hoc test, (C and D) Welch's t-test, or two-way independent ANOVA including group (g) and sex (s) as fixed factors with Bonferroni-corrected pairwise comparisons. Bars and error bars show means and SEM, respectively, with individual data points superimposed.

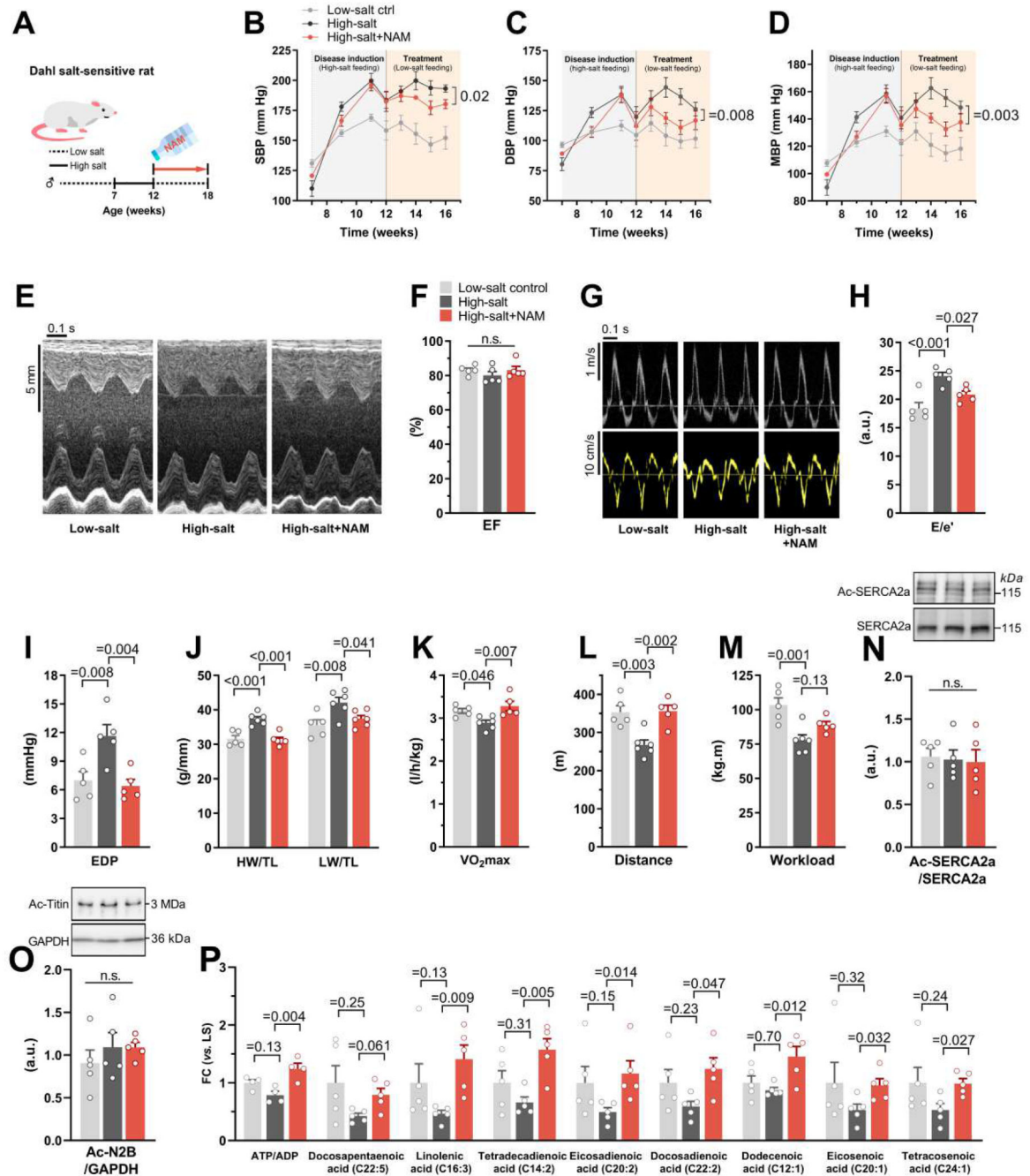


Fig. 6. NAM improves diastolic dysfunction in hypertensive *Dahl* rats.

(A) Schematic representation of nicotinamide (NAM) supplementation to hypertensive *Dahl* salt-sensitive rats. Seven-week-old male rats were fed a high-salt diet (8% NaCl) for 5 weeks followed by treatment in the form of a single intraperitoneal injection of furosemide (10 mg/kg body weight) and a shift to low-salt diet (0.3% NaCl) combined with 40 mM NAM in the drinking water (high-salt+NAM) or not (high-salt). Healthy controls were fed the low-salt diet throughout the experiment (low-salt ctrl). (B) Systolic, (C) diastolic and (D) mean arterial blood pressure, non-invasively measured by the tail-cuff method. (E) Representative

echocardiography-derived M-mode tracings, (F) left ventricular ejection fraction (EF), (G) representative pulsed-wave Doppler (*top*) and tissue Doppler (*bottom*) tracings, and (H) ratio of peak early Doppler transmitral flow velocity (*E*) to myocardial tissue Doppler velocity (*e'*). (I) End-diastolic pressure (EDP) invasively measured by intracardiac catheterization. (J) Heart weight (HW; *left*) and lung weight (LW; *right*) normalized to tibia length (TL). (K) Maximal oxygen consumption (VO₂max), (L) running distance, and (M) workload during exercise exhaustion testing. (N) Representative Western blot (*top*) and quantification (*bottom*) of cardiac SERCA2a acetylation (normalized to total SERCA2a expression), and (O) titin acetylation (normalized to GAPDH). (P) Relative abundance of cardiac unsaturated fatty acids differentially regulated by NAM in 18-week-old *Dahl* salt-sensitive rats, (*n*=4-6 rats per group). *P* values were calculated by (B to D) factorial repeated measures ANOVA (including age and groups as fixed factors) followed by Games-Howell post-hoc test or (F and H to P) ANOVA with Dunnett's post-hoc test. Bars/line and error bars show means and SEM, respectively, with individual data points superimposed.

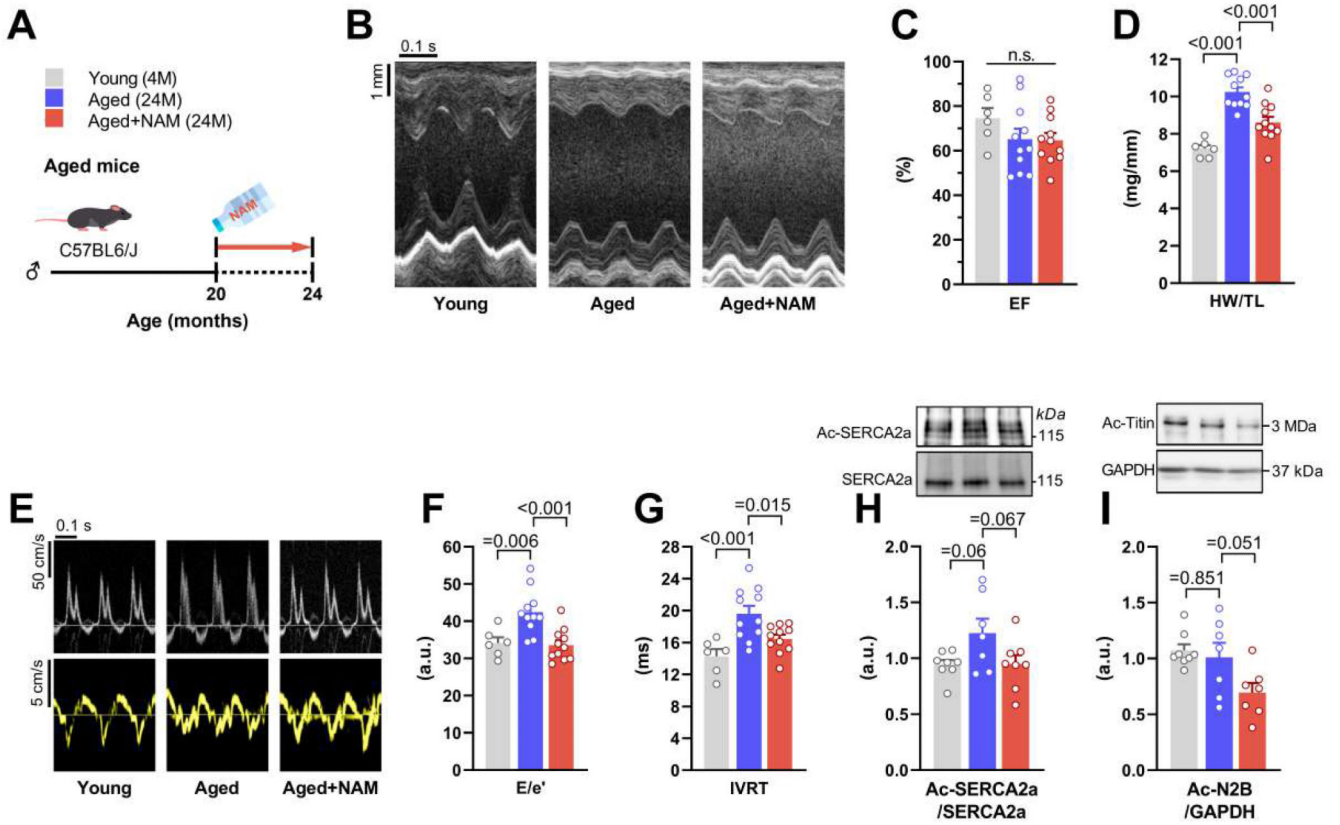


Fig. 7. NAM attenuates age-related diastolic function decline in C57BL/6J mice.

(A) Schematic overview of nicotinamide (NAM) feeding protocol to 24-month-old C57BL/6J male mice. NAM (24 mM) was added to the drinking water starting at the age of 20 months, and after 4 months cardiac parameters were assessed as shown. (B) Representative echocardiography-derived M-mode tracings, and (C) left ventricular ejection fraction (EF). (D) Heart weight normalized to tibia length (HW/TL). (E) Representative echocardiographic pulsed-wave Doppler (*top*) and tissue Doppler (*bottom*) tracings, and measures of diastolic dysfunction, including (F) the ratio of peak early Doppler transmitral flow velocity (*E*) to myocardial tissue Doppler velocity (*e'*) and (G) isovolumic relaxation time (IVRT), ($n=6/11/11$ mice in young/aged/aged+NAM). (H and I) Representative Western blot (*top*) and quantification (*bottom*) of (H) cardiac SERCA2a acetylation (normalized to total SERCA2a expression), and (I) titin acetylation (normalized to GAPDH), ($n=7-8$ mice per group). *P* values were calculated by ANOVA with Dunnett's post-hoc test. Bars/line and error bars show means and SEM, respectively, with individual data points superimposed.

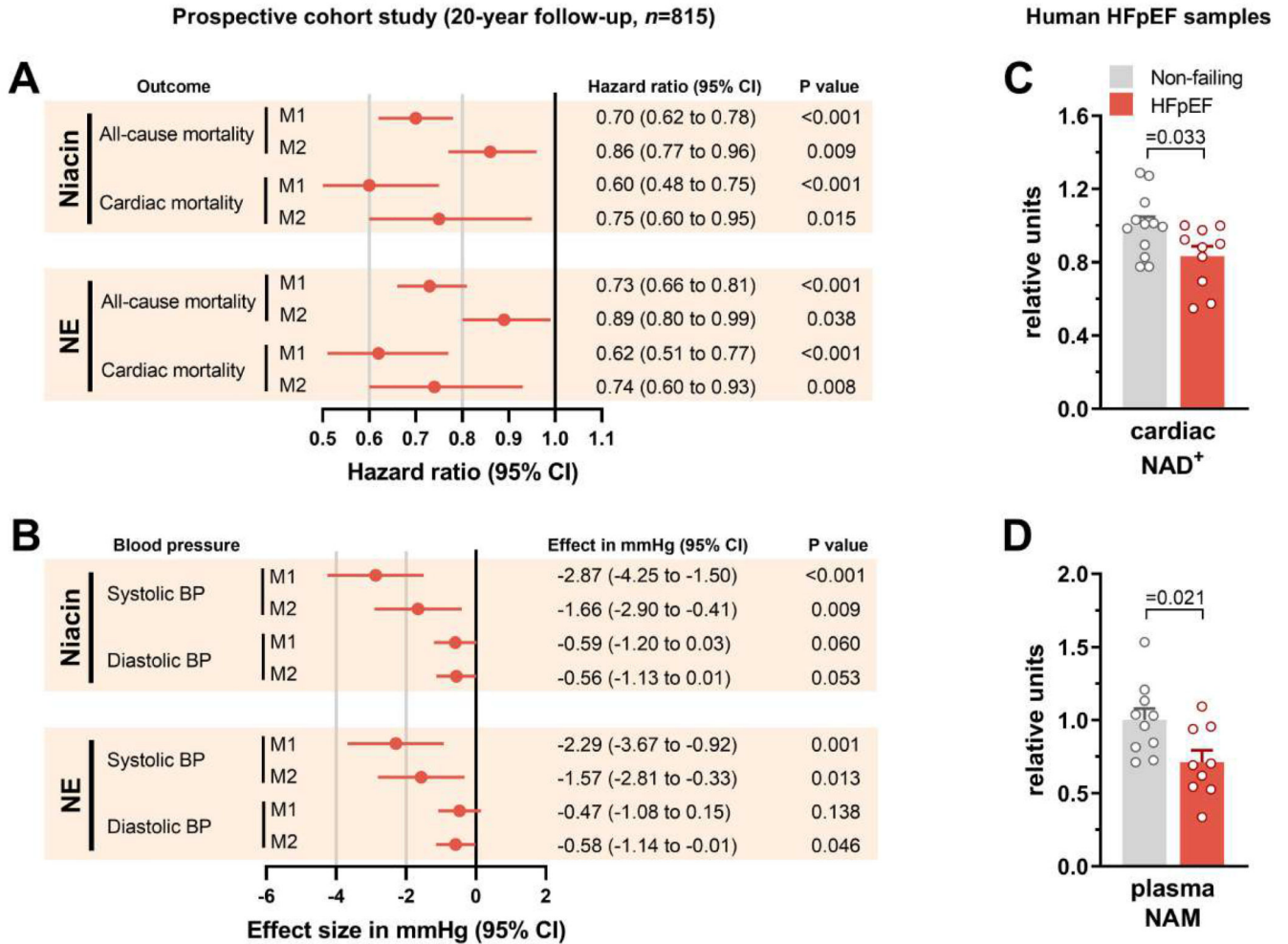


Fig. 8. Higher NAD⁺ is associated with lower risk of HFpEF and cardiac death in humans.

(A and B) Association of baseline (year 1995) dietary intake of niacin and niacin equivalents (NE) with (A) all-cause ($n=335$) and cardiac ($n=77$) mortality during a 20-year follow-up (1995-2015) or (B) systolic and diastolic blood pressure in the Bruneck Study ($n=815$).

(A) Hazard ratios and (B) effect sizes were calculated for a 1-SD unit increase of calorie-adjusted loge-transformed niacin or NE intake. Model 1 (M1) was adjusted for total caloric intake; Model 2 (M2) was additionally adjusted for age, sex, current smoking, diabetes, alcohol intake, hypertension, body-mass index and total cholesterol. (C and D) Relative abundance of (C) cardiac NAD⁺ and (D) plasma NAM in human HFpEF and non-failing hearts ($n=12/10$ and $10/9$ samples, respectively, in non-failing and HFpEF). Bars and error bars show means and SEM, respectively, with individual data points superimposed. *P* values were calculated by (A) Cox regression analysis, (B) linear regression analysis or (C and D) Welch t-test.